FE Modelling of porous structures using Selective laser melting

Author

NS Hamza Ali

Regn Number

00000205033

Supervisor

Dr. Khalid Mahmood

DEPARTMENT OF MECHANICAL ENGINEERING

COLLEGE OF ELECTRICAL AND MECHANICAL ENGINEERING (CEME)

NATIONAL UNIVERSITY OF SCIENCE AND TECHNOLOGY (NUST)

ISLAMABAD

JUNE 2020

FE modelling of porous structures using Selective laser melting

Author

NS Hamza Ali

Regn Number

00000205033

A thesis submitted in partial fulfillment of the requirements for the degree of

MS Mechanical Engineering

Supervisor

Dr. Khalid Mahmood

Thesis Supervisor's Signature: 

DEPARTMENT OF MECHANICAL ENGINEERING

COLLEGE OF ELECTRICAL AND MECHANICAL ENGINEERING (CEME)

NATIONAL UNIVERSITY OF SCIENCE AND TECHNOLOGY (NUST)

ISLAMABAD

JUNE 2020

DECLARATION

I certify that this research work titled "***FE modelling of porous structures using selective laser melting****"* is my own work. The work has not been presented elsewhere for assessment. The material that has been used from other sources it has been properly acknowledged / referred.

Signature of Student

NS Hamza Ali

00000205033

LANGUAGE CORRECTNESS CERTIFICATE

This Thesis has been read by an English expert and is free of typing, syntax, semantic, grammatical and spelling mistakes. Thesis is also according to the format given by the university.

Signature of Student

NS Hamza Ali

00000205033

Signature of Supervisor

(Dr. Khalid Mahmood)

PLAGIARISM CERTIFICATE (TURNITIN REPORT)

This thesis has been checked for Plagiarism. Turnitin report endorsed by Supervisor is attached.

Signature of Student

NS Hamza Ali

00000205033

Signature of Supervisor

COPYRIGHT STATEMENT

ACKNOWLEDGEMENTS

I want to thank Allah almighty who has given me the strength and courage to achieve my goal. I want to thank my parents who were always there for me through every thick and thin. Especially, i want to thank my thesis supervisor ***Dr. Khalid Mahmood*** who helped me throughout my journey. Due to his continuous guidance and support during my research work, i was able to complete my thesis. He always motivated me whenever i was passing through difficult times. He is more than a teacher for me who helped me in achieving my goal.

DEDICATION

Dedicated to

My beloved parents and teachers

ABSTRACT

Selective laser melting is the branch of additive manufacturing in which parts are made layer by layer using laser beam as a heat or energy source to melt the powder layers and manufacture the part according to the CAD model. It has the ability to manufacture highly complex parts which are very difficult to manufacture using conventional techniques. SLM is very popular technique to manufacture orthopaedic implants for the medical industry. If the human bone is damaged, then orthopaedic implants can be installed as a substitute in the human body to ensure quality life for the person. Implants manufactured using SLM have very high elastic modulus as compared to human bone which can cause stress shielding and damage the human bone and so elastic modulus of the implants needs to be lowered. For this purpose, in this research work, we have designed many implants using gyroid and diamond TPMS structures that have elastic modulus close to the human bone, are biocompatible and have good mechanical properties. All the implant designs were inspected and their results were compared and validated with the existing literature. All the designed implants in this research work meet the requirements of an ideal orthopaedic implant and can be physically installed in the human body.

Table of contents

List of Figures

List of Tables

Chapter#1

Introduction

1.1 Research background

Selective laser melting is an additive manufacturing process. It is a powder bed fusion process which utilizes a high intensity laser source and selectively melts powder in particular regions and builds the part layer by layer and according to computer aided design (CAD) data.

When the high intensity laser beam is incident on the build platform where part is to be made layer by layer and where a layer of powder is present, It melts the powder due to the high intensity of the laser beam and first layer of the part is made. The laser source stops for a little while, the formed layer is cooled down and the build platform is lowered. Similarly the second layer of the part is made adopting the same previous procedure and this process continues until the whole part is fabricated layer by layer.

Once the part is made, the excessive unused powder is removed from the build platform and the part is removed either manually or by using electrical discharge machining. If it requires some post processing operations, then they are performed to make the part ready for use. During the building process in selective laser melting, the build platform is usually filled with nitrogen or argon gases to provide an inert atmosphere and to protect the part to be built from oxidation. In some selective laser melting processes, a pre-heating process is performed on the substrate plate or sometimes it is performed in the whole build chamber.

The materials used in selective laser melting are mostly metals. Most common metals used for SLM are iron, titanium and nickel. Moreover, aluminium, tungsten, copper and other metals and alloys are also used in selective laser melting. These materials are cost effective and also have wide industrial application. These materials are usually chosen according to the requirements of desired strength, ductility, bio compatibility etc in the final parts.

Selective laser melting also has applications in the medical field. Orthopaedic implants are also made from SLM process and it has brought a revolution in the field of orthopaedic implants because the implants made from selective laser melting are bio compatible to the human body and also their properties can be tailored to the original human bone i-e cortical and trabecular bone by using suitable materials. So, selective laser melting process is considered as the backbone of medical industry when it comes to the manufacturing of orthopaedic implants.

The need of an orthopaedic implant has increased exponentially specially in the last two or three decades. Its market is expanding globally with a very fast pace. The patients are going towards the medical orthopaedic implants to ensure their quality of life and to perform the daily physical activities with ease. Selective laser melting has made it very easy for the orthopaedic implant developers to manufacture bone implants of good quality.

1.2 Aim of the work

FE modelling of porous structures using selective laser melting will be done in this research work. Different designs of orthopaedic implants will be developed in this work and their results will be compared and validated with the existing literature.

Chapter #2

Literature Review

In this chapter, a detailed research background will be presented about selective laser melting, which is a branch of additive manufacturing. A literature review will be given about the proposed research work, how much work has been done in this field and what work has been done including the future prospects and recommendations by the researcher's who have worked in this field. Problem statement will be identified and then different procedures or ways to overcome the shortcomings and to fill the research gap will be discussed. All the literature will be related to the proposed thesis topic.

2.1 What is Additive manufacturing

First of all the main question is what is additive manufacturing. Additive manufacturing is a process in which parts or components are built in a layer by layer manner using computer aided design data. This CAD data can be prepared using any relevant software. (Ian Gibson et al., 2010).

From a CAD representation to the final part, there are a number of steps involved. The Additive manufacturing steps involved in the production of a part are as follows: (Ian Gibson et al., 2010)

- First of all, a CAD representation of the part is done. It can be done using any suitable software.
- This CAD representation is then converted to a STL file format. Nearly all additive manufacturing machines accept STL file format.
- This STL file is transferred to the AM machine and any required manipulation is done and size, Position, orientation etc are adjusted.
- Now Machine setup is done and different process parameters like layer thickness, hatch spacing, scan speed etc. are given to the machine.
- Now comes the build process. It is usually an automated process but is monitored to look for any errors during the build.
- After the part is build, it is removed from the platform either manually or by using Electrical discharge machining (EDM).
- The part manufactured by AM machine is usually not ready for use and it requires some post processing operations to be performed. Several operations such as sand blasting, polishing, heat treatment etc. are performed before the part is given green signal to be used practically.

- Finally, the application of the part comes, where part is used physically. For example if the part made is a cup, then it can be used for the tea.

These are the eight basic steps involved in the manufacturing of a part usually in all the AM machines.

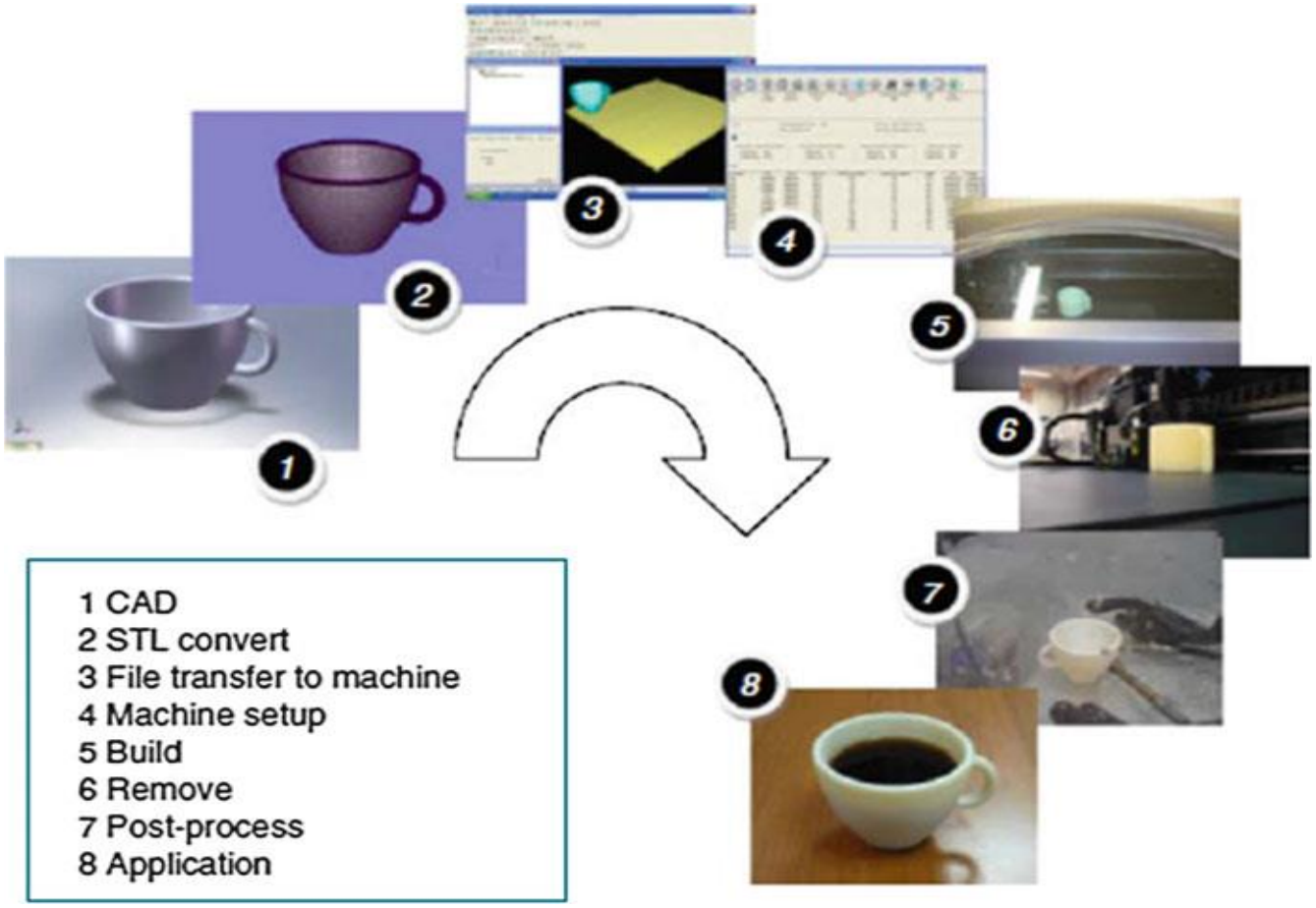

Figure 2-1 Additive manufacturing steps (Ian Gibson et al., 2010)

2.2 Selective Laser melting (SLM)

Selective laser melting is a powder bed fusion process. It is a branch of additive manufacturing process. It uses a high intensity laser beam to melt the powder particles and make parts layer by layer using computer aided design data. This process is different from selective laser sintering which involves partial melting of the material instead of full melting in SLM and also selective

Laser sintering usually uses polymers as materials instead of metals. Selective laser melting is the main topic of this research work, so it will be discussed in detail in this chapter.

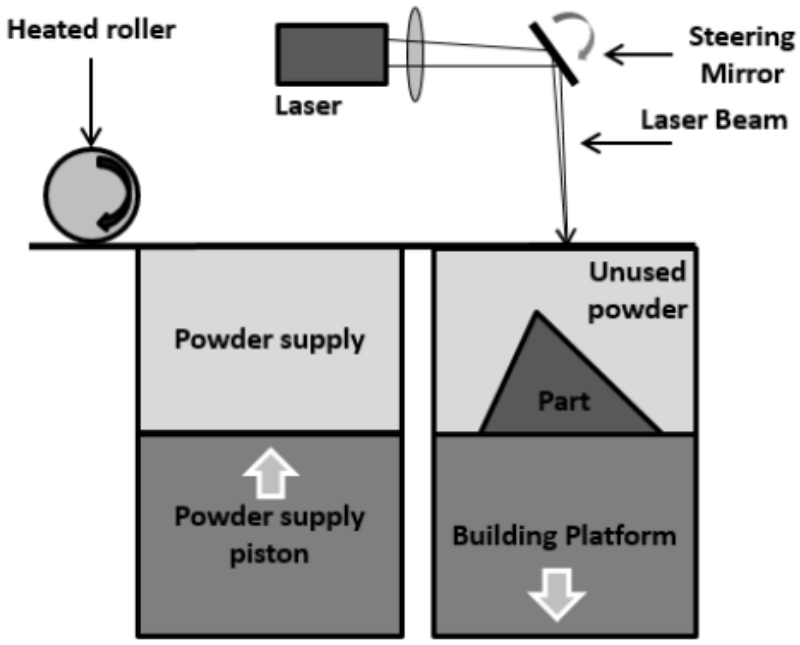

Fig 2-2 Selective laser melting (Bikas et al., 2015)

Selective laser melting process was developed by Dr. D. Schwarze, Dr. M fockele, Dr. W. Meiners, and Dr. G. Andres. For the production of Parts by SLM, process parameters such as hatch spacing, layer thickness, scan speed, laser power etc. are adjusted to get the optimum results [1]. The process of selective laser melting is completely automated other than when the part is removed manually after production with the help of Electric discharge machining.

In the above figure of selective laser melting, the process layout of selective laser melting is described. Heated roller is used to produce a smooth layer of the powder being laid. Powder supply piston is used to supply the required powder quantities. A laser beam is used as an energy or heat source which is directed to the build platform with the help of steering mirror. When the first layer of the part is made, the build platform is then lowered by a thickness equal to that of a layer so that next layer could be made onto the previous one and hence the whole part is fabricated layer by layer. The part is surrounded by the unused powder, which can be separated at the end of the process [2].

2.2.1 SLM physical phenomena

As the selective laser melting process involves the melting of the powder material, it is very important to keep in account the absorptivity of the powder material when laser beam is incident on the powder particles [3]. Thermal fluctuations during the build process should also be considered which results in:

- Balling phenomena
- Crack formation
- Key hole effect
- Melt pool variations
- Part failures

Absorptance is actually the ratio of energy flux that is absorbed by the material to the energy flux incident on the material [3]. Keeping in view the importance of absorptance in selective laser melting, one more factor that is very vital in SLM is process parameters like scan speed, laser power, hatch spacing etc.[3]. All of them directly affect the volumetric energy density that is needed to heat up and melt the powder to manufacture the part. The process parameters involved in selective laser melting are described in the following figure[3]:

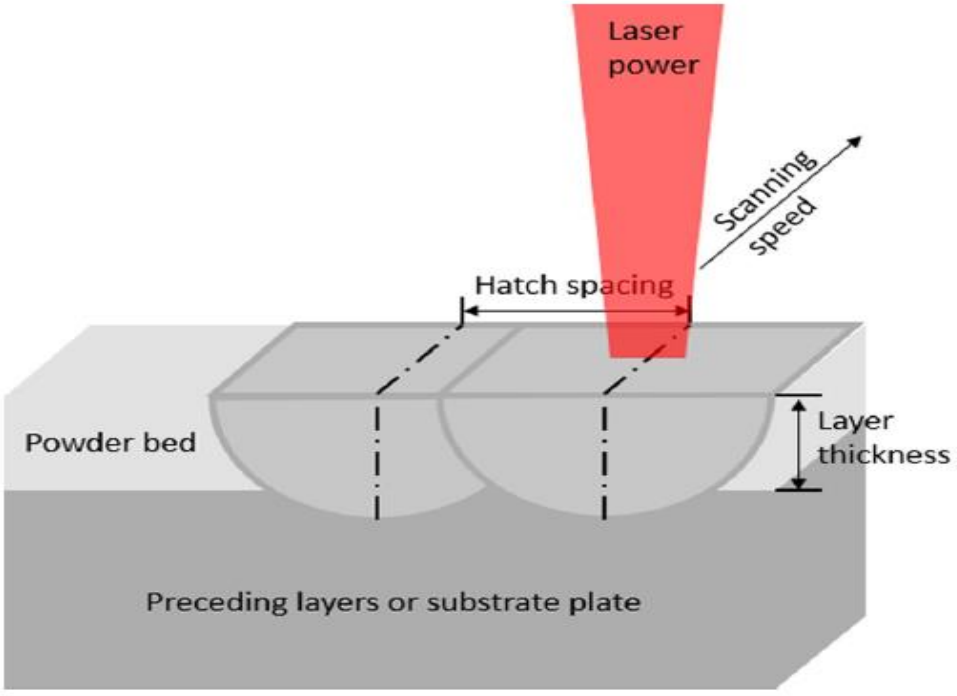

Fig 2-3 SLM process parameters [3]

Absorptivity of different materials is different upon laser irradiation. In case of powder materials, laser beam is irradiated on thin powder surface, So the absorptivity of that powder material can be very much different as compared to the absorptivity of same material in bulk form [3].

Tolochko studied about the absorptance of the powder materials when $C0_2$ infrared radiation is irradiated on them [4]. The absorptance of the bulk material is very less as compared to the absorptance of powder particles of the same material [9]. For example the absorptance of titanium material in bulk form is 30%, on the other hand, the absorptance of titanium powder is 77% which is a big difference when we compare it with bulk titanium [4].

One of the reasons why absorptance of powder material is greater than that of bulk material is the multiple reflections of the laser beam in case of powder materials. These multiple reflections happen through the powder bed and also results in greater penetration depth resulting in higher absorptivity [5]. In their work, Kruth and Gusarrov performed a comparison between the absorptance of bulk materials and absorptance of powder bed and collected the experimental data. This experimental data was then matched with specular reflection model and diffuse reflection model [6]. This model predicts the absorptance of powder bed on the basis of absorptance of bulk material as shown in fig 2-4 [6].

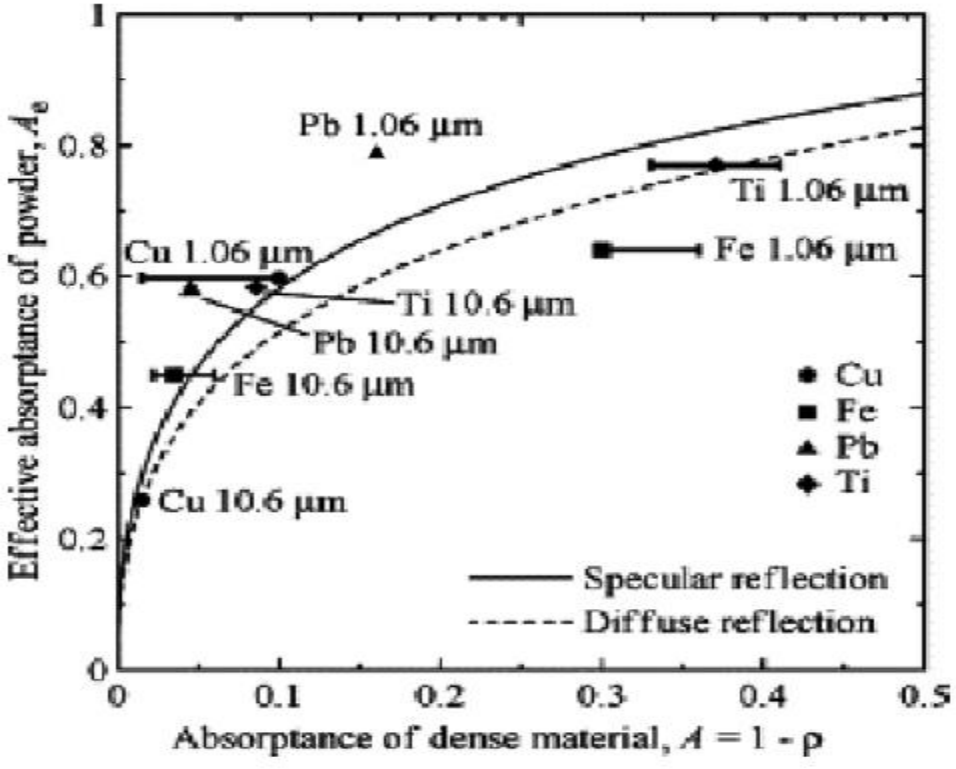

Fig 2-4Effective absorptance of powder bed vs absorptance of bulk material [6]

Several research works have been performed to determine the effects of energy distribution profiles of laser beams on the powder bed. *Loh et al.* concluded that a uniform beam of laser can obtain a larger melt width as compared to non uniform laser beam. It is recommended that a uniform beam of laser should be used in order to get high productivity in selective laser melting process [7].

In another study, Hopkinson and Mumtaz studied the process of SLM using Inconel 625 material using a pulsed laser [8]. Pulsed laser has the capacity to adjust the laser pulse for different pulse frequencies, pulse shapes and also the pulse durations, So it adds an extra dimension of the process control in selective laser melting [8]. Surface roughness of the top surface was lowered using a ramp down pulse shape, but on the other hand it was damaging for the side surfaces. In addition to this, the scanning speed of the system was limited to 400mm/s by using pulsed laser [8].

Powder size and distribution also affects the SLM build process. *Bourell et al*. In his work concluded that smaller 316 stainless powder particles require low energy density and can produce parts that are relatively dense [9]. Liu et al. In his work concluded that the smaller powder particles have the capacity to build more dense parts and they require low laser energy intensity to make parts and the parts built have good surface finish [10]. They have good flow ability and also can get tightly packed with each other resulting in a part that is more strong and durable [10].

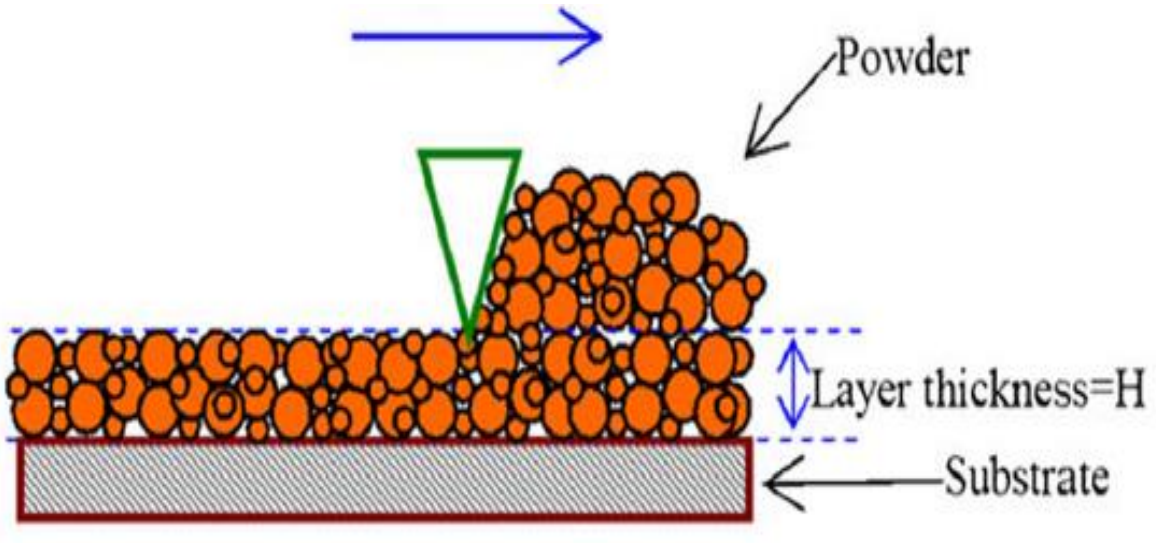

Fig 2-5 Powder layer paving [3]

Balling

In this part, the defect of balling will be discussed in light of the literature review. In selective laser melting, sometimes due to insufficient wetting, spheroidal balls or beads are formed from the molten metal. This phenomenon is known as balling [11]. Due to balling, bead shaped rough surfaces are formed which damages the layers and severely damages the whole SLM process and is detrimental for the part [11].

Li et al. in his work studied the balling phenomena and he concluded that the defect of balling can be significantly reduced by keeping the oxygen level to 0.01%. Furthermore, by using a combination of high laser power and low scanning speed or by rescanning the powder layer can reduce the balling phenomena [12].

Kruth and das et al. also worked on the balling defect and they concluded that an oxide film on the previous layer affects the bonding with next layers and results in the balling defect [13]. It also induces thermal stresses and the poor bonding between the layers also results in delamination. So keeping the oxygen levels to the minimum and the repeated irradiation or exposure from the laser source can be very useful to break the oxide layer and hence avoiding the balling defect [13].

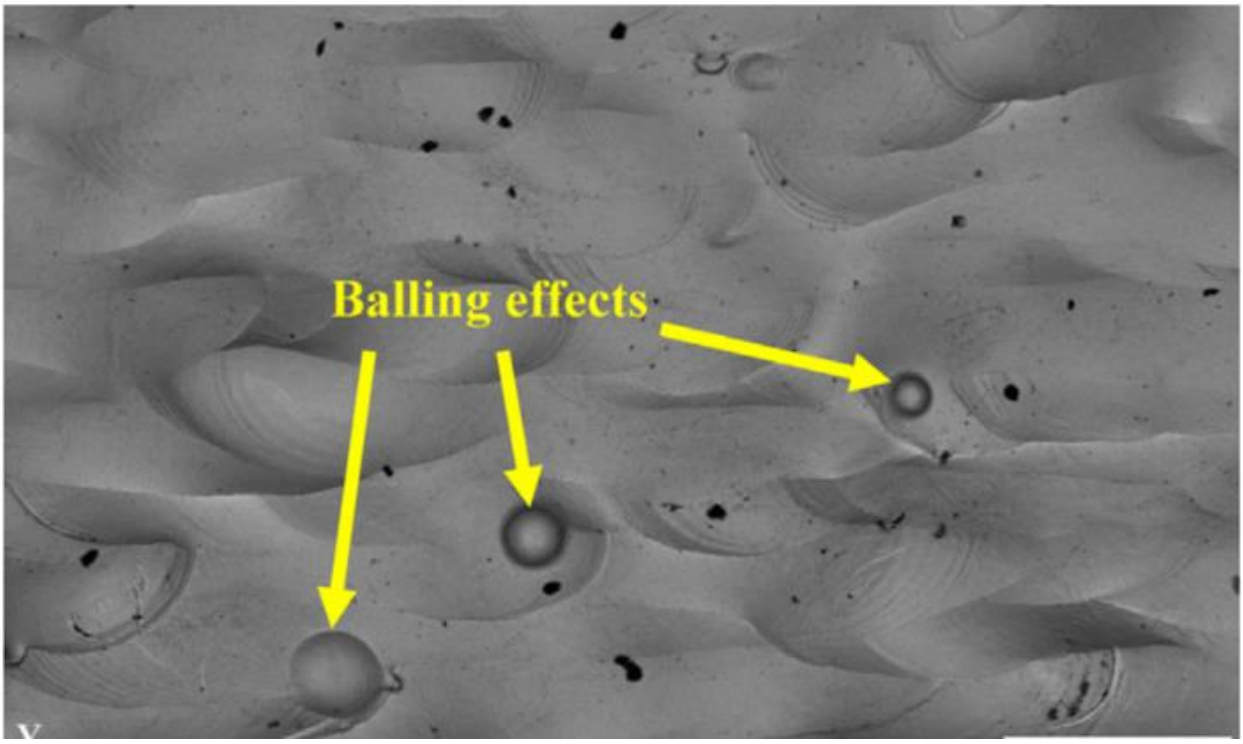

Fig 2-6 SEM images of Balling defect [14]

2.2.2 SLM setup components

Selective laser melting consists up of three parts [15]:

- Laser system
- Powder bed
- Spreading system

Laser system is responsible for heating and melting of powder and consists up of:

- A laser
- Scanner

The powder bed usually consists up of a container which contains the powder from which the part is to be made and it has adjustable height to lower itself for laying the next layer. Spreading system consists up of a powder spreading feeder along with a roller which helps to level off the spread layer in order to get a smooth layer of powder [15].

2.2.3 SLM process parameters

Selective laser melting process consists up of several processing parameters which affect the quality of part and its mechanical properties. These processing parameters are listed below [15]:

- Laser power
- Scanning speed
- Hatch spacing
- Scan pattern
- Scan angle
- Vector length
- Wavelength
- Beam spot size
- Laser energy density

Among all these laser parameters, scan speed, laser power and hatch spacing are considered to be most important process parameters which greatly affect the quality and mechanical properties of the final fabricated part [15].

Laser Power

A laser should have sufficient laser power to melt down the powder layer and form a melt pool of desired size. As the laser power affects the overall process of selective laser melting, so it should be chosen wisely to get the optimum results [15].

Scan speed

Scan speed is also considered as one of the most important process parameter in SLM. Scan speed should be chosen wisely and optimum scan speed should be used for best results. If the scan speed is very high, then the powder layer gets very less interaction with the laser beam which results in incomplete melting (Ian Gibson et al., 2010), [15].

Similarly, if the scan speed is too low, then the powder layers get more interaction time with the laser beam and so it can result in over melting of the powder layers which damages the quality of final part. So, as mentioned earlier, Optimum scan speed should be used for best results [15].

Hatch spacing

In SLM, the distance between melt lines that are adjacent to each other is referred to as hatch spacing. Hatch spacing, scan speed and laser power work in combination for transferring energy from the laser beam to the powder bed. All these process parameters should be selected with care for getting best results[15].

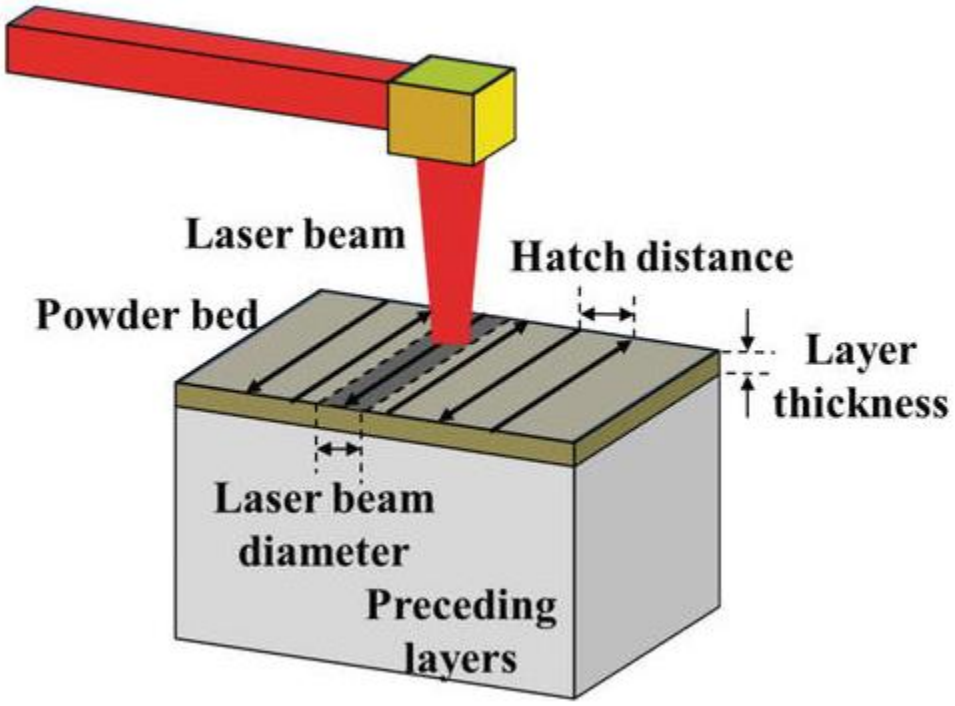

Fig 2-7 Laser beam diameter, hatch distance, layer thickness [15]

2.2.4 Materials in SLM

Materials used in SLM are mainly metals which are listed below [15]:

- Iron
- Titanium
- Titanium Alloys
- Nickel
- 316 Stainless steel
- Cobalt chromium
- cpTi
- NiTi
- Inconel 718
- Tungsten
- Gold
- Aluminium
- Tantalum
- Silver
- Alumina
- Silica

2.2.5 Applications of SLM

The use of selective laser melting process is growing very fast across the globe and it is bringing a new revolution in the field of additive manufacturing due to its ability to produce parts with very complex internal features with great precision and accuracy. Some of the applications of SLM are listed below: [16]

- Industrial tooling
- Heat exchangers
- Turbine blades
- Jet engines
- Furnace fixtures
- Light weight aerospace structures
- Porous scaffolds
- Repair of damaged parts
- Automotive industry
- Jewellery industry
- Dental implants
- Orthopaedic implants

2.3 Porous Metal implants

In recent years, the fabrication of porous metal implants or orthopaedic implants using selective laser melting has been greatly increased. The orthopaedic implants that are very difficult or nearly impossible to produce using conventional techniques are now possible to fabricate using selective laser melting while keeping in mind the: [17]

- Biocompatibility
- Mechanical properties
- Biodegradability
- Porosity levels

Complex structures including bio mimicry features can be fabricated using selective laser melting. This research work is also focused on designing porous metallic implants using selective laser melting. Bone is considered as the main part of our body. It provides: [17]

- Structural support to our skeleton
- Protects tissues and organs
- Stores vital minerals
- Help in performing physical actions
- Stability

Whenever the human body receives some physical injury, then bones have the self healing ability and also have the regenerative property so that with time, it heals the injury. But in case of some severe physical injury, it is very difficult for the human body to recover from the injury because the bones are severely damaged in this case. Moreover, with the age, bones become weaker and so the old people may experience many bone defects. Here comes the need of an orthopaedic implant to fix the damaged part of the bone. [17]

So the need of an orthopaedic implant has increased exponentially specially in the last two or three decades. It's market is expanding globally with a very fast pace. The patients are going towards the medical orthopaedic implants to ensure their quality of life and to perform the daily physical activities with ease. Total knee replacement also known as TKR is also increasing in demand. Between 1991-2006, the demand of total knee replacement has been increased across the globe. [18]

The major demand of total knee replacement is in patients having age between 45-64 years. For example, in the United States, patients with the same age limit spent over US$9 billion for total knee replacement in the year 2009. [19] In 2012, the total value of the biomaterials market was around US$94.1 billion which increased to US$134.3 billion in 2017 globally. [20]

The increase in the value of the biomaterials market across the globe has enhanced the development of bone tissue engineering also known as BTE. In the last few decades, the structural designs and fabrication methods of orthopaedic implants are greatly improved and also new biomaterials suitable for the implants have been discovered. The bone structure consists up of hydroxyapatite crystal which is actually a mineral form of calcium apatite and it is present in an organic matrix of collagen. [21]

95% of this collagen is known as type I, and it provides the structural integrity to the connective tissues present in the bones, ligaments and also the tendons. The remaining 5% of the bone is actually a combination of various non collagenous proteins and also containing proteoglycans. An orthopaedic implant having the desired characteristics will work properly in the human body. On the other hand, an inferior implant can be very damaging for the human body and it can cause serious problems. [21]

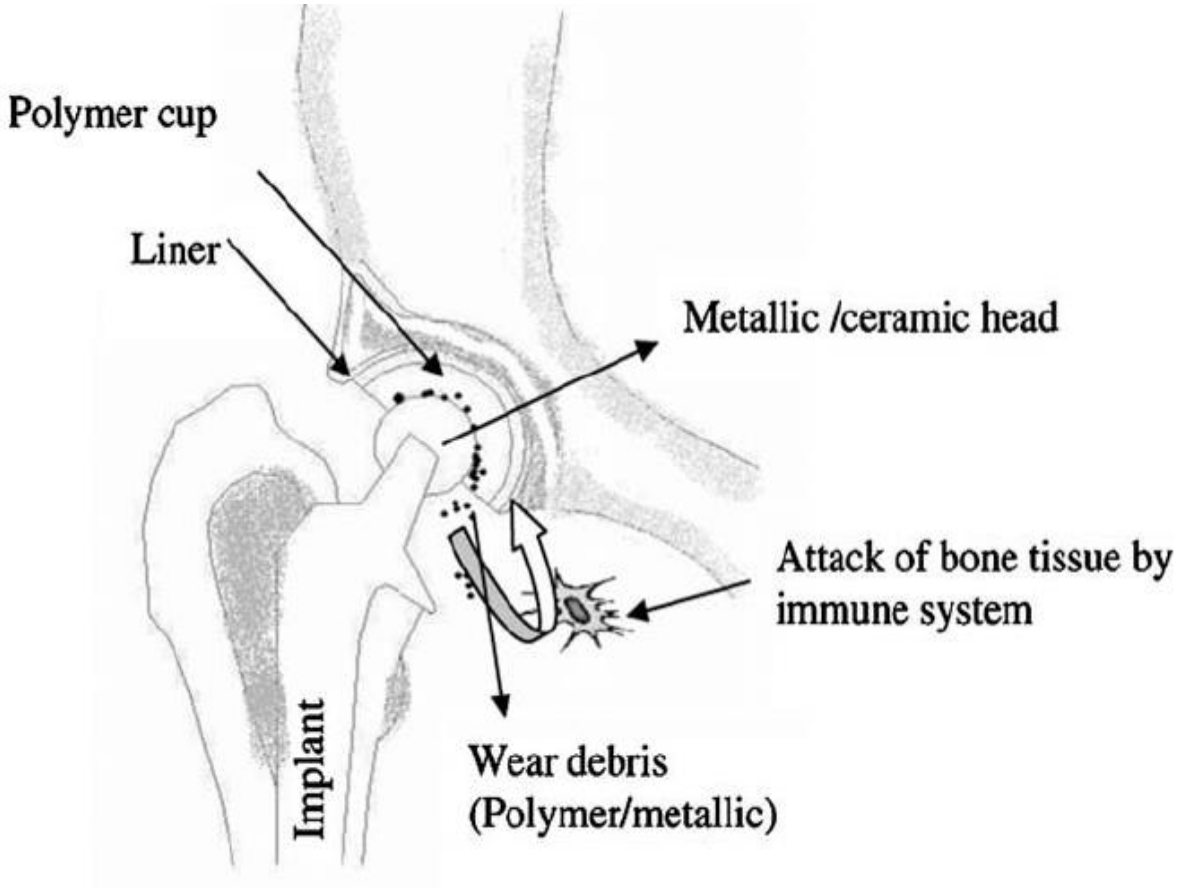

Fig 2-8 Implant in the human body [22]

There are many regulatory authorities across the globe that provide regulatory guidelines for the manufacturers and suppliers of medical implants that what specific characteristics an implant should have to meet the requirements. The implants fulfilling these requirements are given a green signal to be used on the patients. Generally, An orthopaedic implant should have following characteristics: [23]

- Non toxic
- Biocompatible
- Porous structure
- Appropriate porosity levels
- Appropriate elastic modulus
- High strength
- Appropriate compression strength
- Biodegradable in case of temporary implants

All these important aspects should be taken into account while designing and manufacturing the orthopaedic implants. All of these characteristics needed for an effective implant are discussed in detail in the next section.

2.3.1 Requirements for orthopaedic implants

Biocompatibility and non toxicity

An orthopaedic implant should be highly biocompatible as well as non toxic so it does not harm the human body. The materials used for the implants should not have any chemical substances which could damage the cells in the human body so the metallic materials used for the implant should be non toxic. [23]

The level of toxin present in any substance is known as toxicity [24][25]. Metals could be toxic or sometimes cytotoxic. For example metals like cadmium, Mercury and lead are very damaging for the human body and they can damage the cells and organs inside the human body [26]. There are also some metals that are essential minerals for the human body which are listed below [27]:

- Chromium
- Barium
- Iron
- Cobalt
- Lithium
- Selenium
- Beryllium
- Strontium

- Copper
- Boron
- Tungsten
- Molybdenum
- Iodine
- Nickel
- Zinc
- Cerium

On the other hand, excessive amount of these could prove to be toxic [28]. Some of the chemical compounds could chemically break down in the in aqueous conditions like hydrolysis and they may release toxic compounds after the chemical reaction, so they may prove detrimental to human health [29].

There is a very strong relationship between implant material and the human body containing tissues and the living cells. This interaction between the human body and the implant material should be positive resulting in the healing of the wound and the reconstruction of the living cells. So, the implant material that is biocompatible is also sometimes referred to as non toxic which has positive effect on the living cells and also the reconstruction of the tissues [30].

The orthopaedic implant should provide a supportive environment for the tissues and cells activities and obviously this is possible when the implant is biocompatible. Scaffolds in the bone tissue engineering (BTE) act as a template or source for osteogenesis and so the materials used in the scaffolds must be biocompatible with the primary bone cells such as osteocytes, osteoblasts and osteoclasts. This facilitates the formation of new bone, healing and remodelling. [31][32][33]

Biomechanical properties

Load bearing implants make use of metallic biomaterials having following mechanical properties: [34]

- Suitable elastic modulus
- High strength
- Fracture toughness
- Fatigue strength

Titanium and its alloys have all these required mechanical properties so they are widely used in load bearing implant applications. [34]

Implants having high strength support the daily physical activities and also they protect patients from the risks of fracture [35]. If there is a big mismatch between the elastic modulus of the bone and the elastic modulus of the orthopaedic implant, then it can result in stress shielding. Stress shielding is a defect in which the physical stresses are taken up by the orthopaedic implant rather than by the human bone and it can be very detrimental. It is actually a cause of bone atrophy and this may result in the loosening of the implant which finally results in the premature failure of the implant. If the difference between the elastic modulus of bone and the elastic modulus of the orthopaedic implant is small, then stress shielding defect can be avoided. [36]

The human bone is of two types [37]:

- Cortical bone
- Cancellous/Trabecular bone

The outer strong bone is known as cortical bone and it is less porous while the inner porous bone is known as cancellous or trabecular bone. It is much more porous than the outer cortical bone [37].

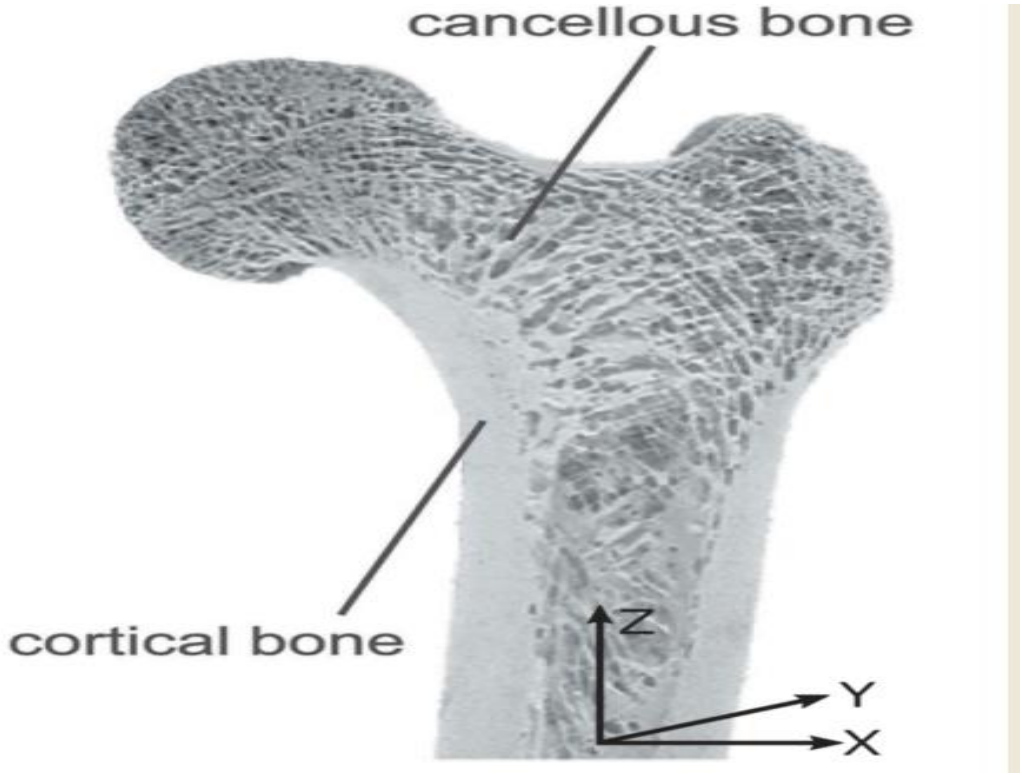

Fig 2-9 Cortical and Trabecular/cancellous bone [38]

The modulus of elasticity of the trabecular or cancellous bone is 1.08 ±0.86 GPA [39], although it varies with the person. On the other hand, the modulus of elasticity of cortical bone ranges from 7.7-21.8 Gpa which is very much higher when we compare it with cancellous bone [40]. So, the orthopaedic metallic implants should have modulus of elasticity close to these ranges, otherwise stress shielding could occur.

In reality, the modulus of elasticity of the metallic implants is much higher as compared to that of natural human bone. For example, the elastic modulus of CP-Ti is 112 Gpa and the elastic modulus of titanium alloy Ti-6Al-4V is around 110 Gpa which is very much higher than the elastic modulus of cortical and trabecular bone, So the elastic modulus of these metals should be lowered to the levels of the human bone for getting an ideal metallic implant that is compatible with the human body [41].

Metal/Alloy	*Density, ρ (g/cm^3)*	*Young's Modulus, E (GPa)*
316L stainless steel		
annealed		
30% cold work	7.9	200
80% cold work		
Co-Cr-Mo alloys	8.3–9.2	210–240
CP titanium	4.5	110
Ti-6A1-4V	4.5	110
Ti-6A1-7Nb	4.7	100
Ti-5A1-2.5Fe	4.5	110
Ti-13Nb-13Zr	5.6	80
55 Nitinol	6.45	70
60 Nitinol	6.71	113

Table 2-1 Modulus of elasticity (E) of different biomedical Alloys [42]

The elastic modulus of different biomedical alloys used in orthopaedic implants are much higher than the modulus of human bone and they can cause stress shielding as well as can give serious damage to the human body. So, their elastic modulus should be decreased to the levels of human bone for an ideal implant compatible with the human body.

Biodegradability for the temporary implant materials

Due to the advancements in additive manufacturing technology and the induction of new designs

For the metallic implants, the requirement of low modulus of elasticity for the implant is almost met using open cellular structures and requirement of new bone tissues ingrowths using metallic implant is also met [43].

As the metallic implants are placed inside the human body, The long term consequences of this should also be kept in mind. For example, in case of temporary implants using biomaterials such as titanium and it's alloys, the material do not degrade with time and it remains inside the body as an hostile object. This can cause many health issues like the infections caused due to bacteria, irritation in the body and also it can cause inflammatory reactions in the human body and so the life of patient is affected [43].

Biodegradable materials can be a good choice to counter above problem. These materials slowly degrade with time and are replaced by the newly formed tissues. Magnesium, iron and zinc based alloys are examples of these biodegradable materials. But, these could only be used for temporary implant applications and their use is limited as mostly non biodegradable materials are used for permanent implants as the mechanical properties of the implant should also be kept in mind as a primary requirement of the implant and medication can be done to counter any simple concerns caused by them [44].

2.3.2 Porosity of the implant materials

In a solid structure, the percentage of void space is known as porosity [45]. Porosity can be calculated as follows:

$$P = (1 - \rho_{structure}/\rho_{material}) \cdot 100\%$$

In this equation, $\rho_{material}$ is the density of the bulk alloy whereas, $\rho_{structure}$ is the density of porous structure and it can be calculated by mass/volume of the structure [46].

Porous structure with appropriate porosity

Bone is also a porous structure and it consists up of cortical bone and cancellous bone. Cortical bone is the outer hard shell of the bone and is less porous, while cancellous bone is the inner bone with high levels of porosity. The porosity levels of cancellous bone ranges from 30% to 95%. Pore size of cancellous bone ranges from 200-1000µm [47][48][49][50].

In recent years, Interest in the development of porous metallic implants having mechanical properties close to that of human bone has been greatly increased. Porous implants not only have modulus of elasticity close to the human bone, but they also support the ingrowths of new bone tissues inside the pores of the implant and also facilitate body fluid circulation [50].

Porosity effect on biocompatibility

Metallic implants with high level of porosity are preferred due to their high biocompatibility and the ability to grow new bone tissues inside the pores facilitating bone regeneration [51][52]. Porosity is considered to be very important in designing metallic implants. Kuboki et al. In his work concluded that osteogenesis occurs only in porous structures [53].

For the purpose of cell distribution and migration and to facilitate blood vessel formation, the porous structure of the implant should be open cellular and interconnected. Minimum pore size should be 100µm which helps in the migration and transportation of bone cells for osteogenesis [54][55]. For the implant to be more biocompatible and to better support the bone tissue ingrowths, the pore size used in implant should be between 200-1200µm.

Porosity effect on mechanical properties

Porosity is inversely proportional to modulus of elasticity. If the structure is highly porous, then its modulus of elasticity will be low [56]. Human bones perform different physical activities in their daily routine and they also experience many mechanical loads in the form of force, stress etc. So the implant should have good mechanical properties to help support daily activities [57]. Titanium alloys are most popular for metallic implants due to their superior biocompatibility and mechanical properties but titanium alloys have much higher modulus of elasticity as compared to human bone which can cause stress shielding. To overcome this, porosity is introduced in the implant structure to minimize the elastic modulus difference between implant and bone and also maintaining the required mechanical properties [58][59][60][61][62][63].

SLM and electron beam melting are the most popular AM techniques to fabricate these porous implants but SLM is preferred over EBM because it results in better quality implants. A comparison between SLM and EBM is shown in table below:

	SLM	EBM
Powder sources	One or more fiber lasers of 200–1000 W	High power Electron beam of 3000 W
Build chamber environment	Argon or Nitrogen	Vacuum/He bleed
Method of powder preheating	Platform heating	Preheat scanning
Powder preheating temperature (°C)	100–200	700–900
Maximum available build volume (mm)	500 × 350 × 300	350 × 380 (diameter × length)
Maximum build rate (cm^3/h)	20–35	80
Layer Thickness (mm)	0.020–0.100	0.050–0.200
Melt pool size (mm)	0.1–0.5	0.2–1.2
Surface finish (Ra)	4–11	25–35
Geometric tolerance (mm)	± 0.05–0.1	± 0.2
Minimum feature size	40–200	100

Table 2-2 SLM vs EBM comparison [41]

2.4 Triply periodic minimal surface (TPMS) structures

Triply periodic minimal surfaces consist up of periodically infinite structure along three independent directions also having zero mean curvature of the surface. TPMS structures are made by repeating the elements with minimum possible area also referred as unit cells. These unit cells combine with each other to get a complete TPMS structure. TPMS structures are considered very vital for porous metallic implants due to their high biocompatibility and good mechanical properties. Implants usually have the problem of high elastic modulus as compared to the human bone therefore causing stress shielding, but by using TPMS structures to build porous metallic implants, the elastic modulus of implant comes very close to that of human bone and so avoiding the stress shielding problem [64][65].

TPMS structures also help in the new bone tissues ingrowths inside the pores of the implant thus supporting new bone formation and tissues growth. Therefore, in order to get an ideal implant that is highly biocompatible having good mechanical properties and also having modulus of elasticity close to that of human bone, TPMS structures are the best design till date to manufacture an ideal orthopaedic implant. Some of the TPMS structures include gyroid, diamond, D-prime surface and neovius surface. Gyroid and diamond TPMS structures are considered to be more popular to build quality implants [66].

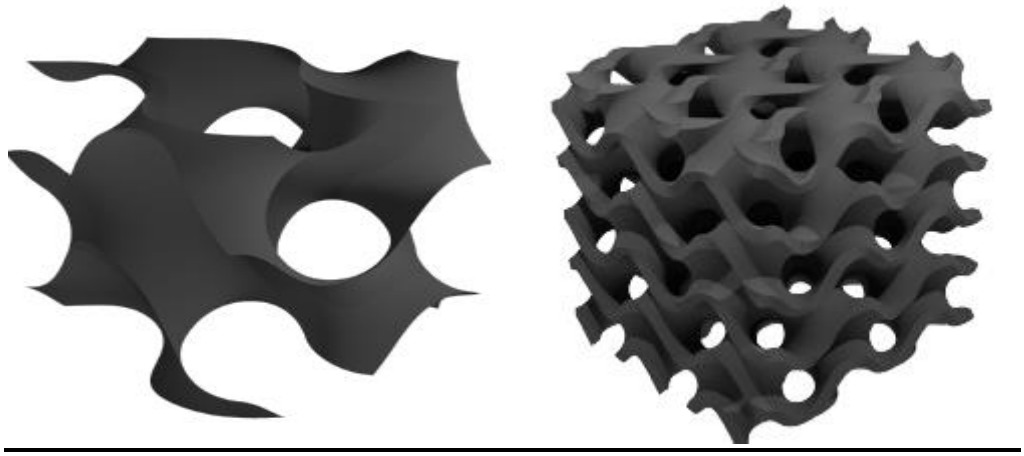

Fig 2-10 TPMS unit cell and structure [67]

TPMS architecture can be represented in a strict mathematical equation which makes its design very convenient. TPMS structures and its design are discussed in detail in the next chapter.

2.5 Literature summary

An orthopaedic implant should Posses:

- Biocompatibility
- Good mechanical properties
- Non toxic
- Biodegradability in case of temporary implants

All of the previous research works faced the problem of stress shielding. In addition, majority of the designs did not have appropriate pore sizes for cells and tissues ingrowths and many faced manufacturability issues.

So, an ideal orthopaedic bone implant was needed to be designed which can:

- Overcome stress shielding
- Have pore sizes suitable for cells ingrowths.
- Biocompatible,
- Have elastic modulus close to the levels of human bone.
- Porosity levels within the ranges of human bone and is manufacturable.

Chapter #3

Design and modelling of orthopaedic implants

3.1 Materials and methods

In this research work, gyroid and diamond TPMS structures were designed for bone implants. TPMS structures have pores that are interconnected with each other just like the human bone. They also facilitate the cells and tissues in growths through the pores which help in bone reconstruction and healing. Pore sizes and porosity levels were selected according to the requirements of human bone. Unit cells were used to design complete lattice structures for bone implants. Material chosen for all the implant designs was Ti–6Al–4V alloy due to its good mechanical properties, biocompatibility, fatigue resistance and has lower modulus of elasticity when we compare it with other metals like stainless steel etc. The design and modeling of these orthopaedic mplants is discussed in detail in the next sections.

3.2 Triply periodic minimal surface (TPMS) structures

As discussed in the previous chapter, triply periodic minimal surfaces consist up of periodically infinite structure along three independent directions and also have zero mean curvature of the surface. These structures are highly porous and their mechanical properties are also in a close range to that of human bone, so they are considered as the best candidates for fabricating orthopaedic implants as they have all the characteristics possessed by the human bone. So, TPMS structures are used as a design for the development of the orthopaedic implants.

TPMS can be defined by implicit functions. Each TPMS architecture can be expressed or represented in a strict mathematical equation. Some of the TPMS architectures defined by a strict mathematical equation are listed below:

Gyroid surface: $$F(x, y, z) = cos(x)\cdot sin(y) + cos(y)\cdot sin(z) + cos(z)\cdot sin(x) + a$$

Schwarz diamond: $$F(x, y, z) = sin(x)sin(y)\cdot sin(z) + sin(x)\cdot cos(y)\cdot cos(z) + cos(x)\cdot sin(y)\cdot cos(z) + cos(x)\cdot cos(y)\cdot sin(z) + a$$

Neovius surface: $F(x, y, z) = 3\cdot(cos(x) + cos(y) + cos(z)) + 4 \cdot(cos(x)\cdot cos(y)\cdot cos(z)) + a$

D − prime surface: $F(x, y, z) = 0.5\cdot(sin(x)\cdot sin(y)\cdot sin(z) + cos(x) \cdot cos(y)\cdot cos(z)) - 0.5\cdot(cos(2x) \cdot cos(2y)\text{þ}cos(2y)\cdot cos(2z) + cos(2z)\cdot cos(2x)) + a$ (8)

Among all of them, gyroid and diamond TPMS are considered as one of the best designs for the orthopaedic implants because their design is compatible with the human bone and also has the mechanical properties very close to that of human bone. So they are the best designs in order to develop an effective and efficient orthopaedic implant.

.

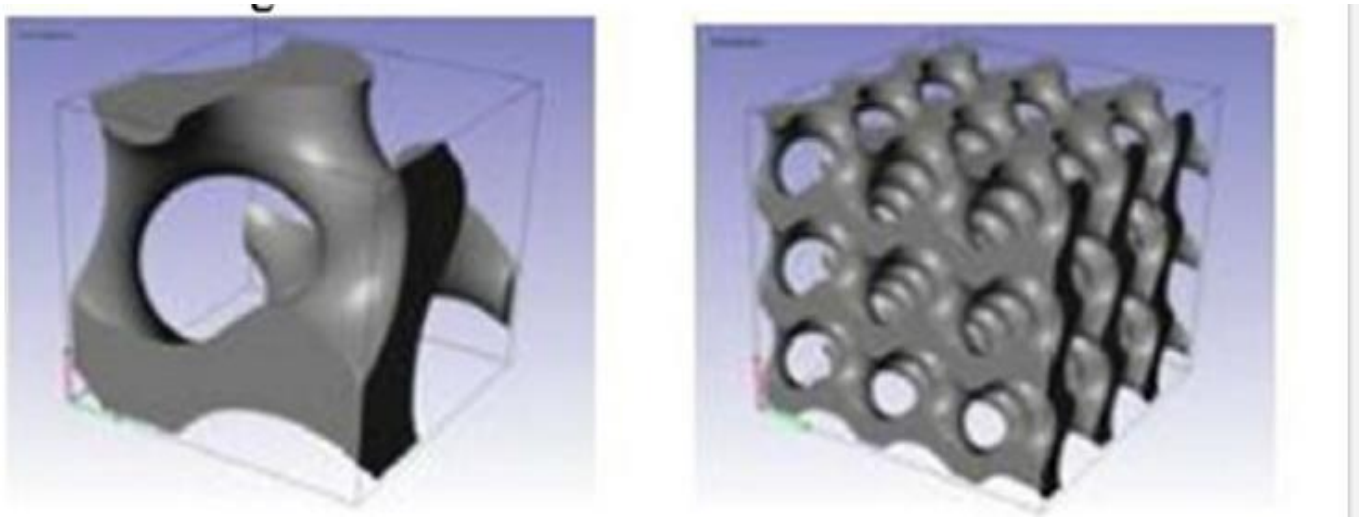

Fig 3-1 Gyroid unit cell and lattice [68]

In the figure 3-1, gyroid unit cell and gyroid lattice is presented. Unit cells combine with each other to form a complete lattice structure.

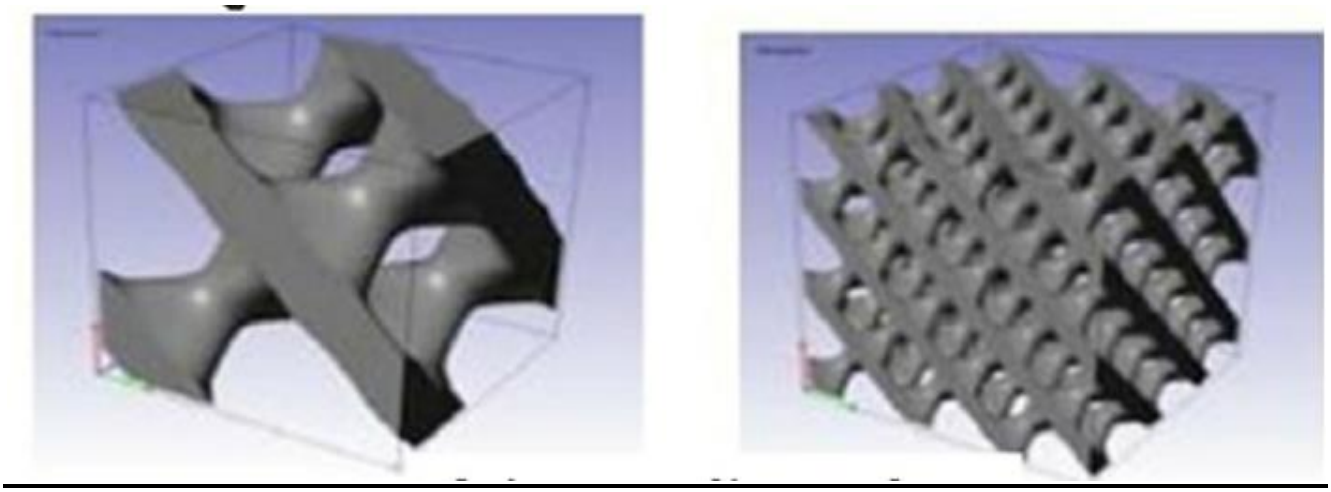

Fig 3-2 Diamond unit cell and lattice [68]

In figure 3-2, Diamond unit cell and lattice structure is presented. Unit cells combine with each other to form a complete diamond lattice structure.

Additive manufacturing has the greater capability of designing and fabricating theses complex porous structures with the help of selective laser melting which is nearly impossible by using conventional manufacturing techniques. Diamond and gyroid TPMS structures are considered to be the best designs for orthopaedic implants. Some the orthopaedic implants using different levels of porosities and materials are presented below in the table:

Structure (Scaffolds)	Porosity (Volume fraction %)	Material
Gyroid	80–95	Ti—6Al—4V
Gyroid	5–10	Ti—6Al—4V
Diamond	80–95	Ti—6Al—4V
Diamond	5–10	Ti—6Al—4V
Gyroid	–	Ti—6Al—4V
Gyroid	82	Ti—6Al—4V
Gyroid	84.5	Ti—6Al—4V
Gyroid	85	Ti—6Al—4V
Gyroid	68.7	CP—Ti (grade 1)
Gyroid	73.3	CP—Ti (grade 1)
Gyroid	72.4	CP—Ti (grade 1)
Cortical bone	5–10	Human bones
Trabecular bone	50–90	Human bones

Table 3-1 Different TPMS structures with varying porosities [41]

From table 3-1, we can see that all of the designs for implants make use of gyroid and diamond TPMS structures and different levels of porosities are being used in them. In this research work, we will also focus on the designs of gyroid and diamond TPMS structures to be used as orthopaedic implants.

The final designed implant using diamond or gyroid TPMS structures consists up of pores that are interconnected with each other and making it a compact design. The final implant design looks like as follows:

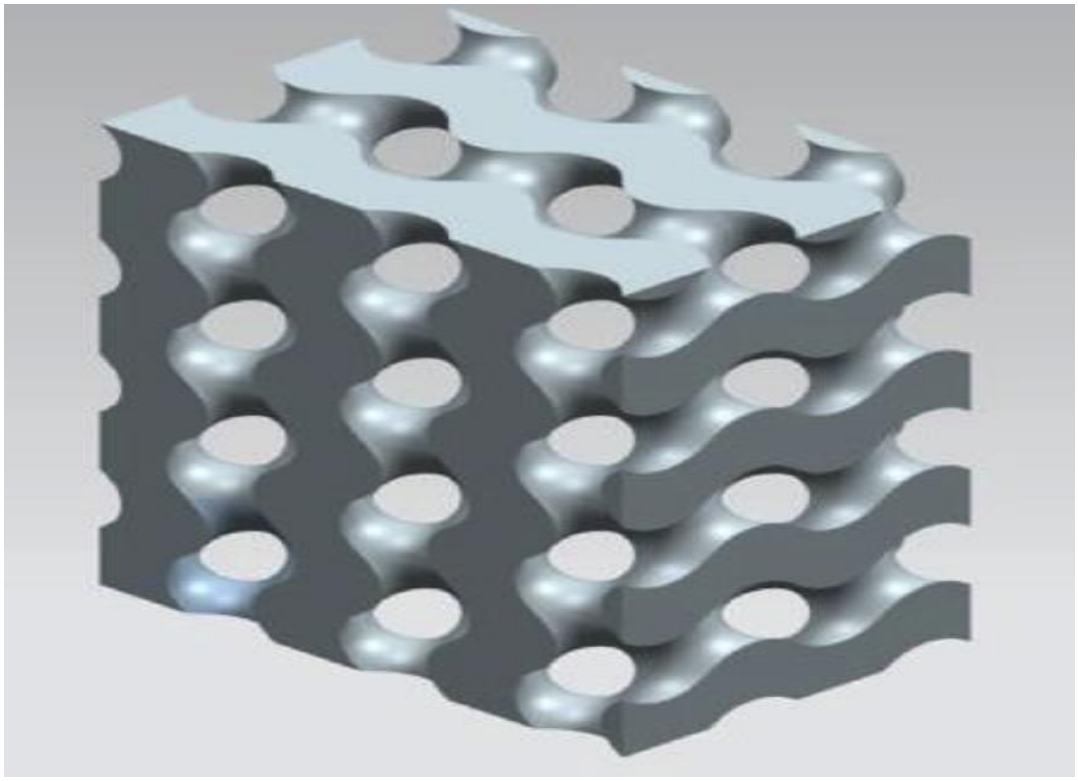

Fig 3-3 TPMS implant [41]

3.3 Design and modelling of our orthopaedic implant

3.3.1 Unit cell generation

The first step involved in designing and modelling of our TPMS structures will be the generation of unit cells. We know that the TPMS unit cells can be represented in a strict mathematical equation.

Gyroid unit cell

$\cos(x)*\sin(y) + \cos(y)*\sin(z) + \cos(z)*\sin(x)$

This equation can be modified as:

cos(x)*sin(y) + cos(y)*sin (z) + cos (z)*sin(x) +a

In this modified equation, ‘a’ is the factor that controls porosity levels. Its value usually ranges between 0-1. By changing the value of ‘a’, we can easily change the porosity levels of the unit cells according to our requirement. If we wish not to use this ‘a’ factor in the equation for the creation of the unit cell, then we can later adjust the porosity levels of structures in mesh magic software that will be discussed later.

To create a unit cell of gyroid, we will use ***MATHMOD 9.1*** Software which gives us utility to create the triply periodic minimal surface unit cells by simply inserting the relevant mathematical equation,

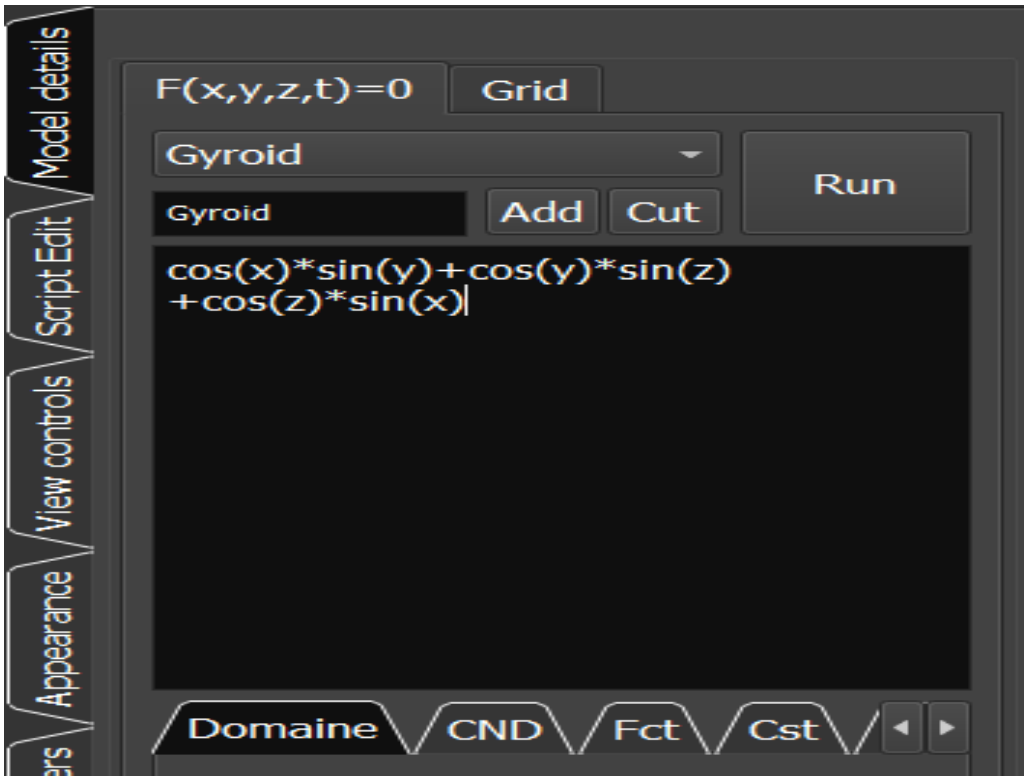

Fig 3-4 Mathmod software window

Fig 3-4 represents the window of mathmod software which is used to create the gyroid unit cell with the help of mathematical equation. The gyroid unit cell created using mathmod is given below:

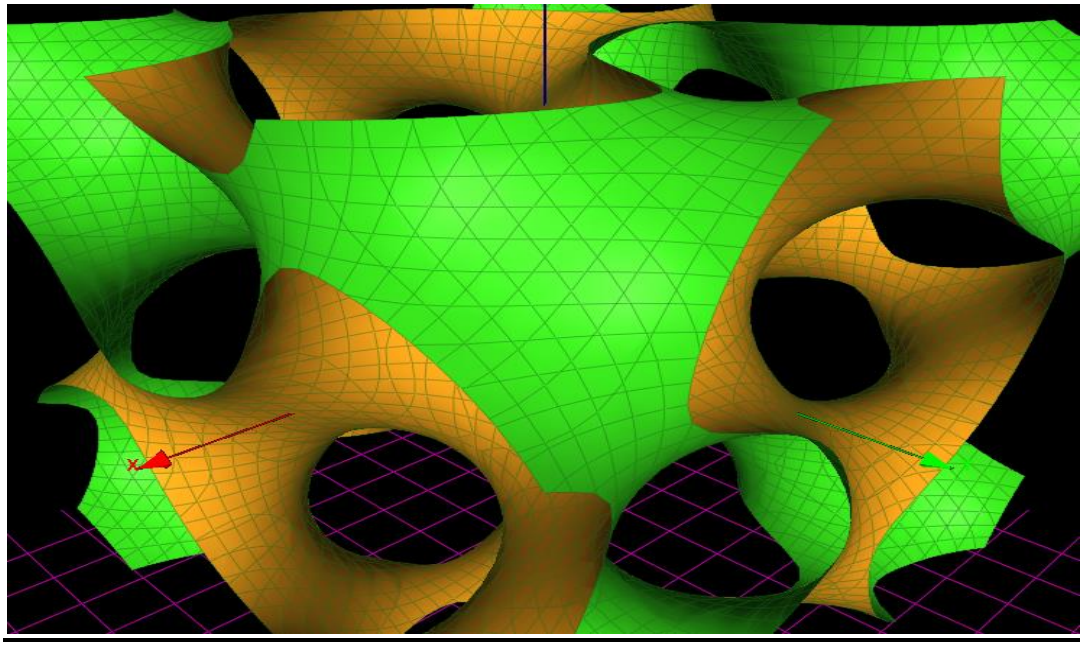

Fig 3-5 Gyroid unit cell created by mathmod

Similarly, by changing the factor ‘a’ in the modified equation, the porosity of the unit cell is also changed and so the shape of the unit cell also changes as below:

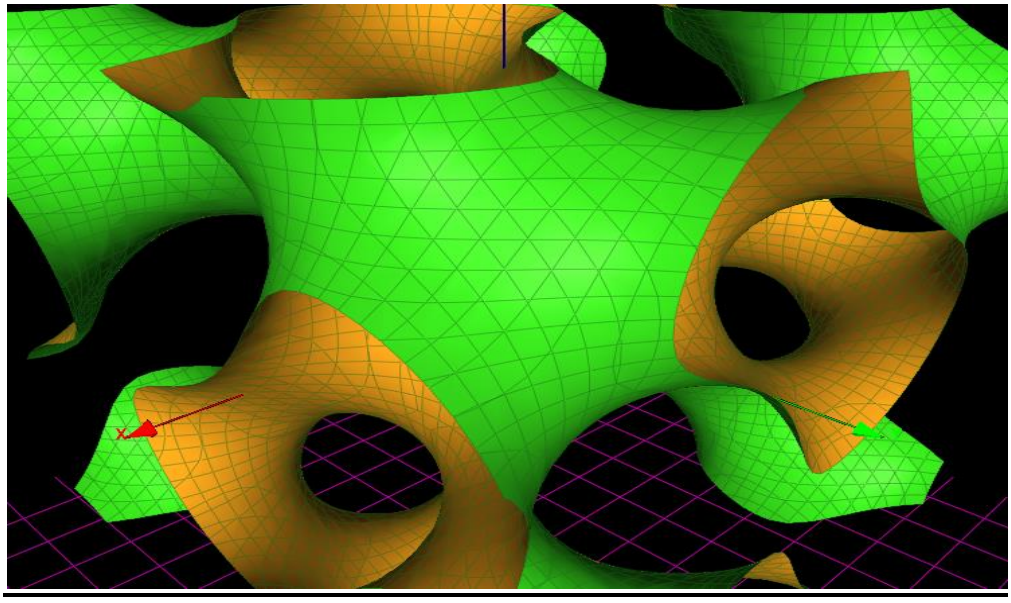

Fig 3-6 Gyroid unit cell with modified porosity

So, we can easily alter the porosity levels of the unit cell by changing the factor ‘a’ and if we wish to do it on a later stage, we can do it by using mesh magic software discussed later.

Diamond unit cell

We know that diamond unit cell can be represented in a strict mathematical equation given below:

sin(x)*sin(y)*sin(z)+sin(x)*cos(y)*cos(z)+cos(x)*sin(y)*cos(z)+cos(x)*cos(y)*sin(z)

Similarly if we want to alter the porosity levels at the unit cell creation stage then we can modify the above equation as follows:

sin(x)*sin(y)*sin(z)+sin(x)*cos(y)*cos(z)+cos(x)*sin(y)*cos(z)+cos(x)*cos(y)*sin(z) + a

Where ‘a’ is the factor that controls the porosity levels as discussed earlier. If we want to control the size of TPMS structure at unit cell level, then we can multiply a factor ‘2π/L’ with x, y and z coordinates of gyroid and diamond unit cell equations, where ‘L’ is the size of unit cell. By inserting the relevant equation of diamond unit cell in the mathmod software, we can get the diamond unit cell which is represented below:

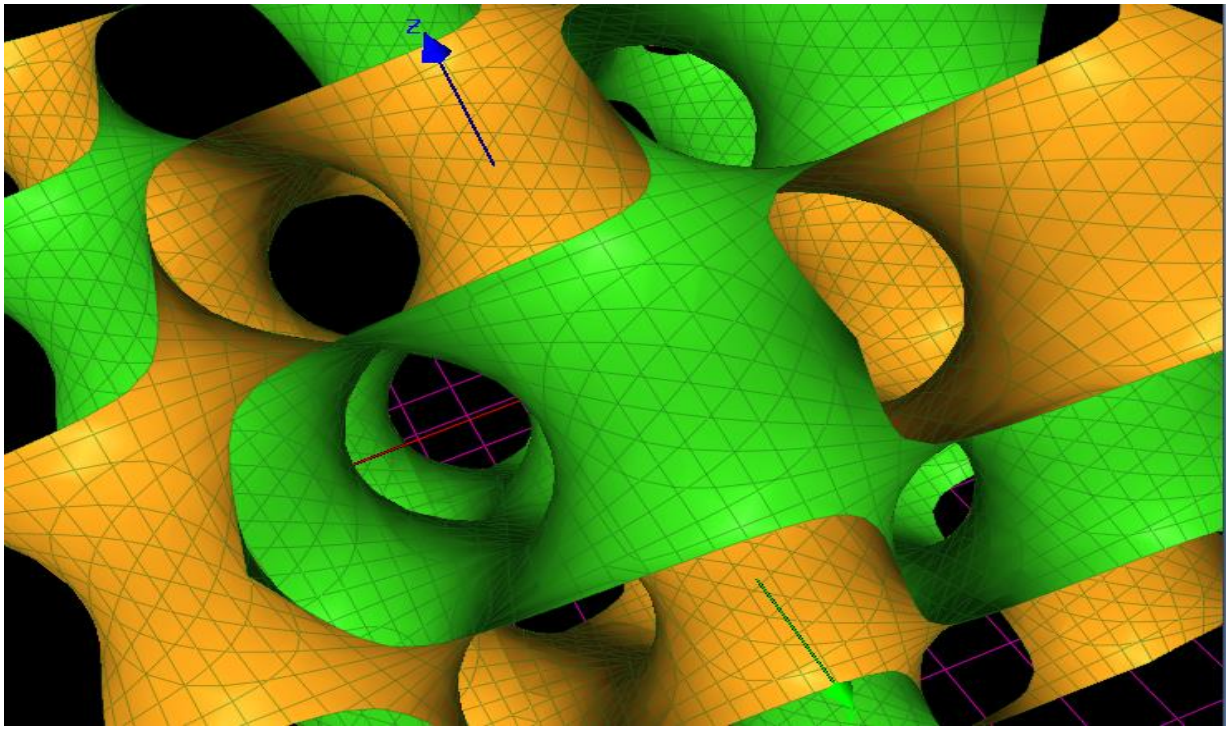

Fig 3-7 Diamond unit cell created by mathmod

Similarly, the porosity levels of the unit cell can be changed at unit cell design stage or it can be altered at the TPMS lattice stage as discussed previously. So, with the help of mathmod, gyroid and diamond unit cells are created.

3.3.2 Converting unit cell to STL format

Once the unit cells are created, they are saved in obj format. This format is then converted to STL file format by using spin 3D by NCH software.

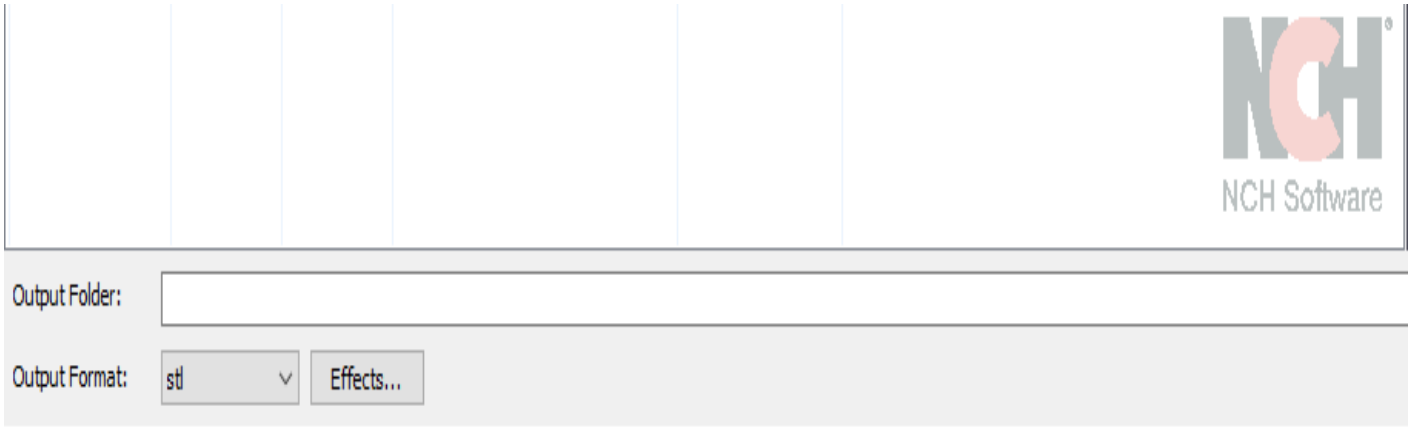

Fig 3-8 Spin 3D NCH software STL file conversion window

Now the unit cell is converted into STL file format and we can manipulate it easily.

3.3.3 TPMS lattice creation

Gyroid lattice

Now, the unit cell is converted into STL file format so we can work on it and create a complete lattice structure by repeating the unit cells in x, y and z directions. For this purpose, we will use *Mesh magic by NCH software*. This software has the utility to convert unit cells into complete lattice structures by offering cell repetitions into x, y and z directions respectively and then converting it from surface to a complete compact solid lattice structure.

Unit cells are repeated in x, y and z directions equally resulting in a complete 3D lattice structure. The dimensions for our first implant design are 9*9*9 mm^3. Mesh magic gives us the utility that if our lattice structure dimensions are less or greater than our requirement, then we can scale down or up our lattice structure to get required dimensions.

Also, mesh magic gives us the utility to change the porosity levels of our lattice structure as well as we can also change the dimensions of our lattice structure. So, by repeating unit cells in x, y and z directions, using scaling and porosity levels changing functions of this software, we can easily get gyroid TPMS lattice structure according to our requirements and it is a compact solid structure saved in STL file format and is compatible with the additive manufacturing printing machines.

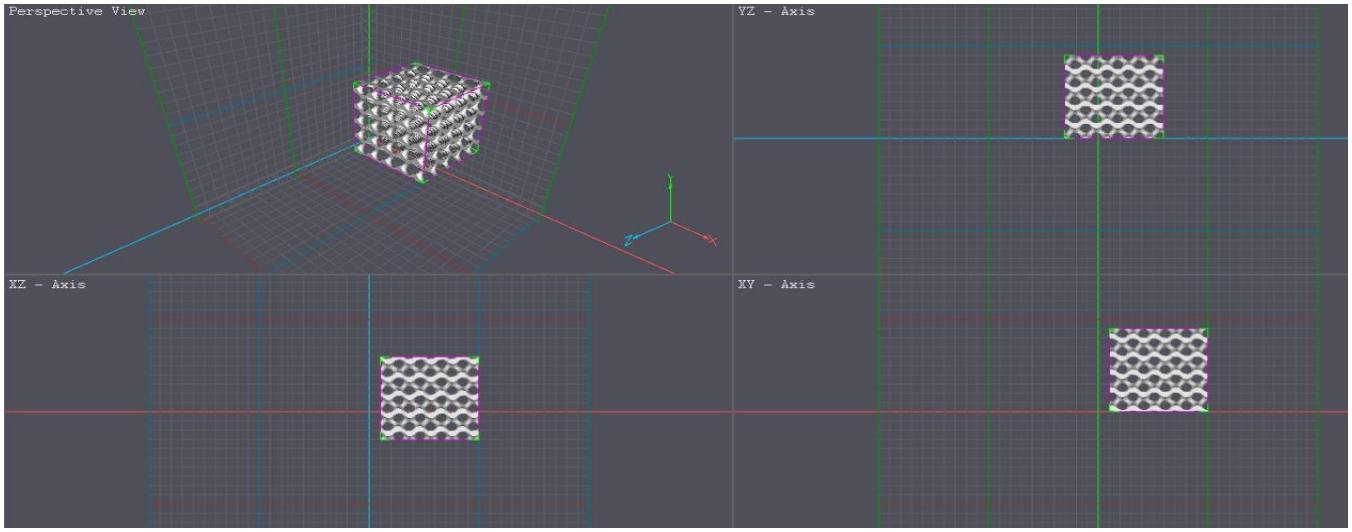

Fig 3-9 Gyroid lattice created by using Mesh magic software

Diamond lattice

Similarly, to create diamond lattice structure, first of all the unit cell that was saved in obj file format using mathmod software is converted to STL file format using spin 3D by NCH software. Now, this STL file is imported into mesh magic software and by repeating unit cells in x, y and z directions and by using scaling and porosity changing functions of the mesh magic software, diamond TPMS lattice is created as a compact solid structure. The same procedure as adopted in case of gyroid lattice was used in the creation of diamond lattice structures. The file is saved in STL file format and is compatible with the AM printing machines.

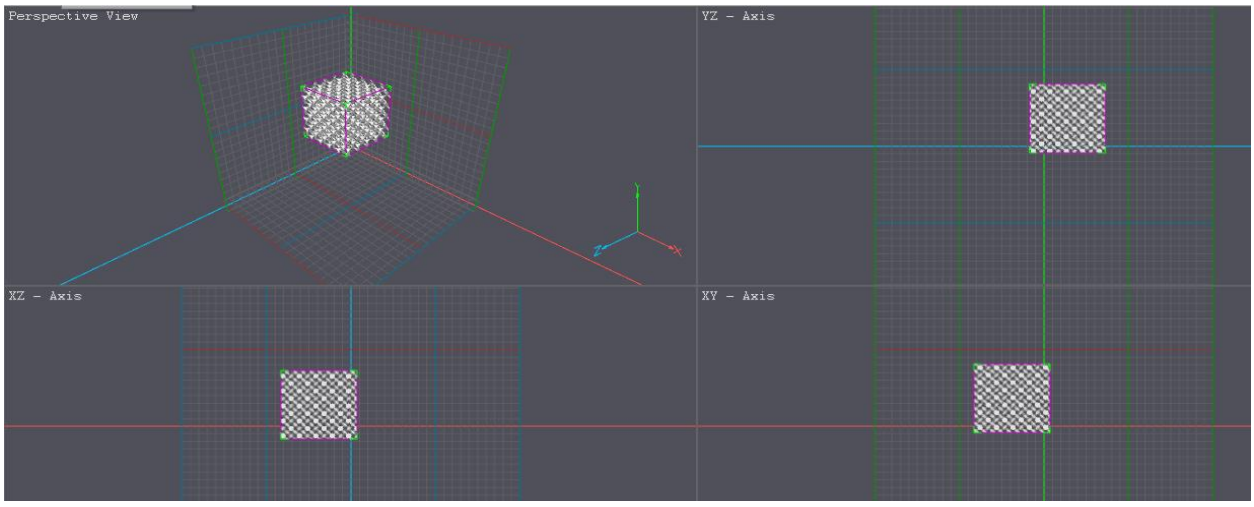

Fig 3-10 Diamond lattice created using Mesh magic software

Diamond lattice structure also has the same dimensions like gyroid lattice structure which are 9*9*9 mm^3 .

3.3.4 Measurements for desired metallic implant

Once the gyroid and diamond lattice structures are created, the most important step of the implant design comes. In this step, the metallic implant is inspected that does it meet the requirements of an orthopaedic implant. The most important feature of the implant is related with pore size which is discussed below:

Pore size of implant

Pore size is considered to be the most important aspect of the implant design, As the orthopaedic implant is installed inside the human body, so it should meet some requirements. Implants are made highly porous to get closer to the mechanical properties of the human bone and also to support the cell and tissues growth. So, the implants should have an appropriate pore size which helps in the cells and tissues growth. The pore size of the implant should range from 200-1250 µm to better support cell and tissue ingrowths.

In this research work, we have designed multiple orthopaedic implants with different dimensions, pore size and porosities while keeping in mind the requirements of human trabecular bone. The first implant design using gyroid and diamond lattice structures was previously discussed. More designs will also be presented in the next section.

Gyroid lattice pore size

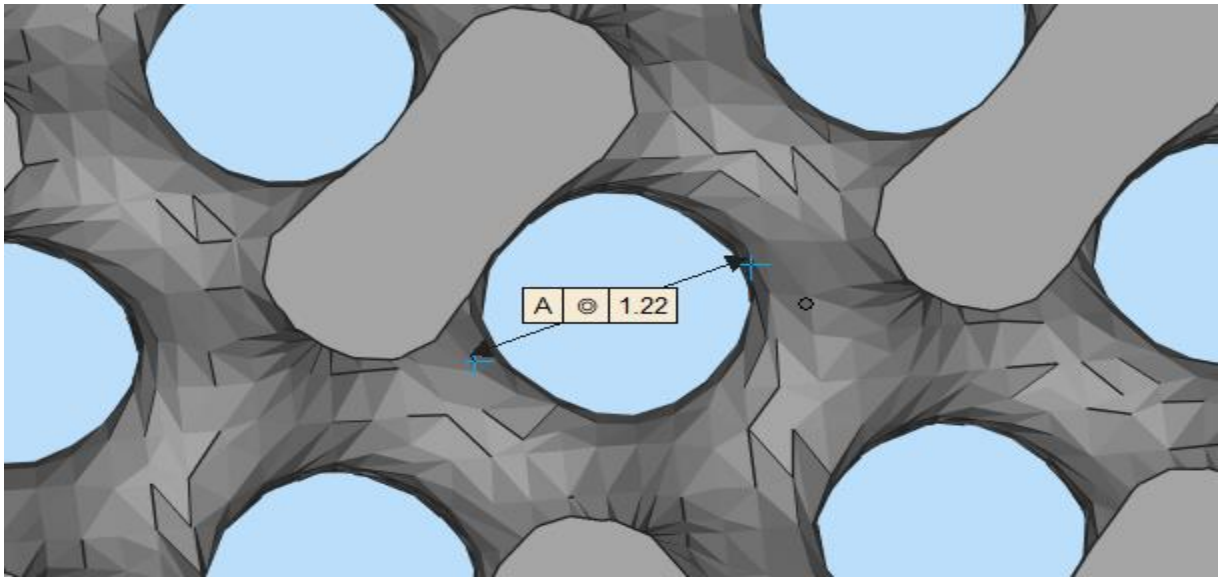

Fig 3-11 Gyroid lattice pore size

In this first design of the gyroid lattice, the pore size is 1.22mm or 1220µm and the overall dimensions of the lattice are 9*9*9 mm^3. So, this design meets the requirements needed for an orthopaedic implant.

Diamond pore size

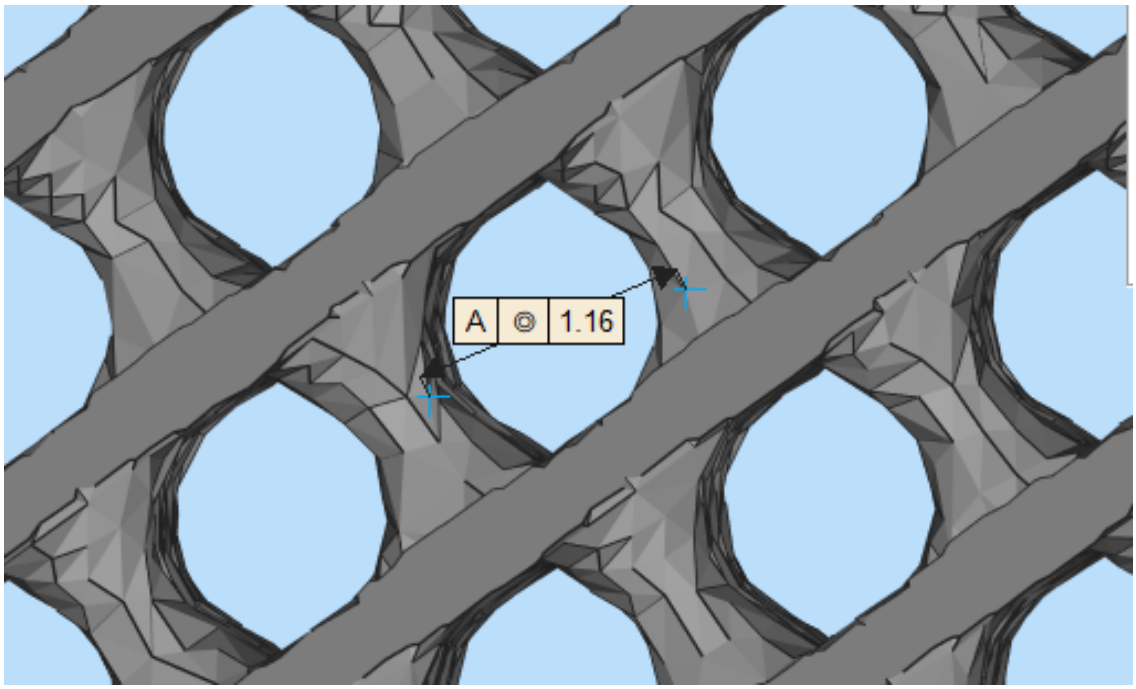

Fig 3-12 Diamond lattice pore size

In this design of diamond lattice structure, the pore size is 1.16mm or 1160µm and the overall dimensions of the lattice structure are 9*9*9 mm^3.So, this design meets the pore size requirement of the orthopaedic implant.

Many other implant designs having different dimensions, pore sizes and porosity levels are also designed in this research work. They are designed by keeping in view the general requirements of an orthopaedic implant.

Once these lattice structures are designed, they are then imported into ANSYS software and simulations are done using a new module of ansys known as ANSYS additive module. All of the steps performed in the ANSYS workbench and the obtained mechanical properties will be discussed in the next chapter. An orthopaedic implant should have all the required properties that are close to the human bone so that it does not act as a hostile element in the human body. Other designs of the orthopaedic implants designed in this research work are presented below in the table.

S.no	Type	Pore size (µm)	Porosity (%)
1	Gyroid	1220	60.45
2	Diamond	1160	69.08
3	Gyroid	780	70.49
4	Diamond	740	79.49
5	Gyroid	620	76.03
6	Diamond	570	80.02
7	Gyroid	440	76.75
8	Diamond	400	84.64

Table 3-2 Different designs created for Orthopaedic implants

Table 3-2 presents different implant designs that are developed in this research work. All of the designs created in this research work meet the requirements of the orthopaedic implants. The trabecular bone has a porosity range of 50-90% [71], so all the implants in this research work are designed having porosity levels between 50-90%. The design process followed in all the implant designs is same as discussed earlier. So, different types of implants are designed in this research work keeping in mind the general requirements of an orthopaedic implant.

3.3.5 Material used for implants

Material chosen for all the implant designs is Ti–6Al–4V alloy. This material is most popular for load bearing implants and also has good mechanical properties, biocompatibility, fatigue resistance and has lower modulus of elasticity when we compare it with other metals like stainless steel etc. So, this material is suitable for all the implant designs.

Chapter #4

Results and validation

4.1 Overview

In this chapter, the results of the simulation work are discussed in detail and the validation of the results with existing literature is done. This chapter covers all the steps involved in the simulation and finally the results and validation part. Implants are inspected at the end whether they have or not the required mechanical properties that are close to the human bone. So, the orthopaedic implant designs suitable for the human bone are recommended.

4.2 Simulations in ANSYS workbench

4.2.1 Importing the part

First of all, the lattice structure that was designed earlier is imported in ANSYS workbench. A new module of ANSYS known as ANSYS additive module is used in this research work. This module is newly launched by ANSYS and it has the utility to model the whole process of selecting laser melting.

This process gives us the results during the whole build process layer by layer so we can easily monitor if there are any problems during any layer in the build process and we can rectify it by removing that problem. This is a huge breakthrough in the field of additive manufacturing which helps us to monitor the whole selective laser melting process during the build stage. If there are any problems during the process, then we can remove those shortcomings and can also alter our design to get the optimum results thus saving cost and money.

The most important thing is that no research work has been done till date using this new module of ansys known as ANSYS additive module. In our research work, this module will be used for the first time ever to model the whole selective laser melting process.

Gyroid TPMS

First of all, the gyroid lattice structure that was designed earlier and is explained in the previous chapter is imported into ANSY workbench additive module. The import file has STL file format that is compatible with the ANSYS workbench additive print module. The imported file of gyroid lattice is shown below.

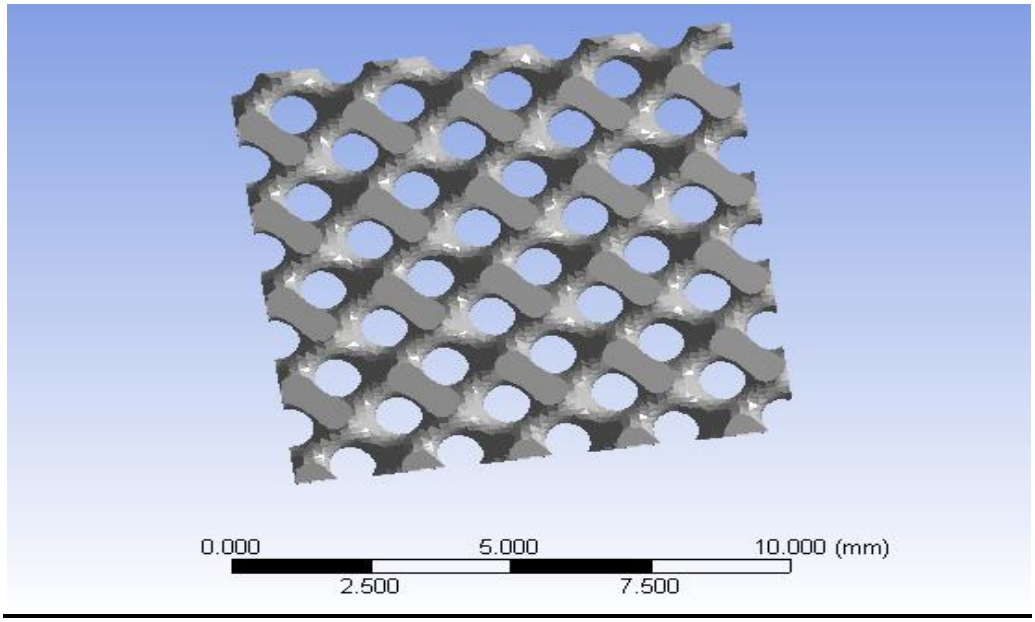

Fig 4-1 Gyroid lattice import in ANSYS

Diamond TPMS

Similarly diamond lattice structure is also imported in ANSYS additive print module. The file format of the lattice structure is STL file format that is compatible with the NSYS additive print module. The imported diamond lattice is shown below:

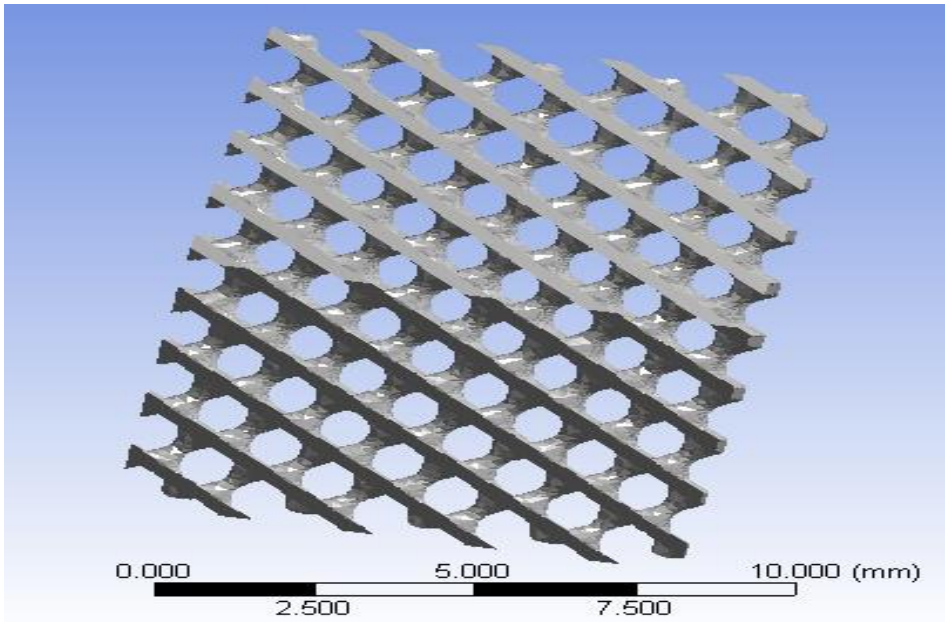

Fig 4-2 Diamond lattice import in ANSYS

4.2.2 Material selection in ANSYS

Once the gyroid and diamond lattices are imported in ANSYS additive module, the next step is to select an appropriate material from the material library of ANSYS. As explained earlier that Ti–6Al–4V alloy is used in all our implant designs due to its good mechanical properties, biocompatibility and lower modulus of elasticity as compared to other metals, so we will chose Ti–6Al–4V alloy from the material library of ANSYS.

Gyroid lattice material selection

Ti–6Al–4V alloy material is assigned to the gyroid lattice structure and is presented below:

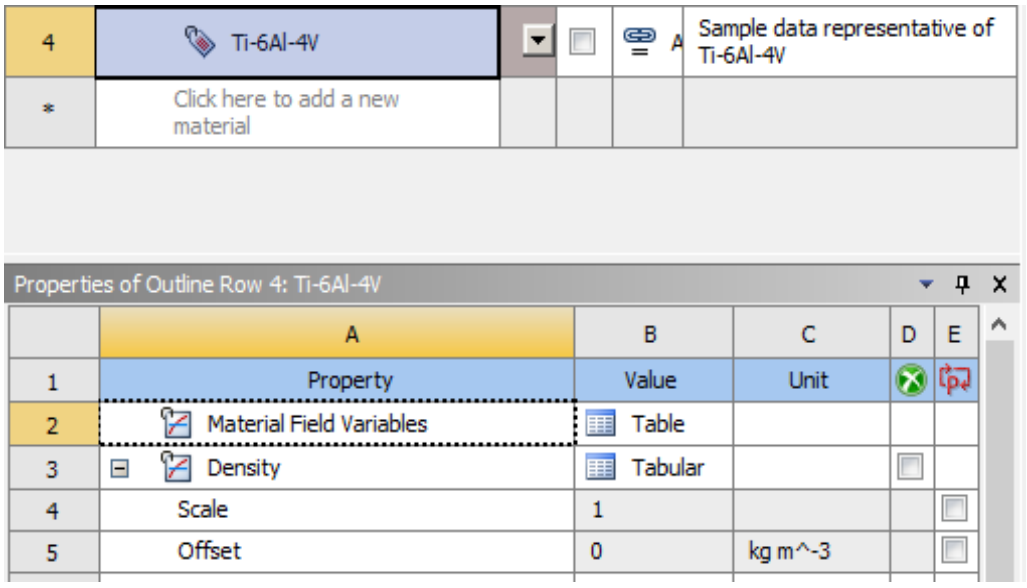

Fig 4-3 Gyroid lattice material assignment

Diamond lattice material selection

Similarly Ti–6Al–4V alloy material is assigned to diamond lattice structure from the material library as explained previously.

4.2.3Base generation

In majority of the additive manufacturing processes, a base or substrate is needed on which the part is manufactured. The base is removed at the end of the build process and part is separated. Selective laser melting also needs a base on which the part is made layer by layer. As the ANSYS additive module gives us the utility to completely design selective laser melting process, so base on which the part is to be made can be created in this module of ANSYS. This base is usually rectangular in shape and is flat.

Base creation for gyroid lattice

Now the rectangular base is created at the bottom of the part which is shown below:

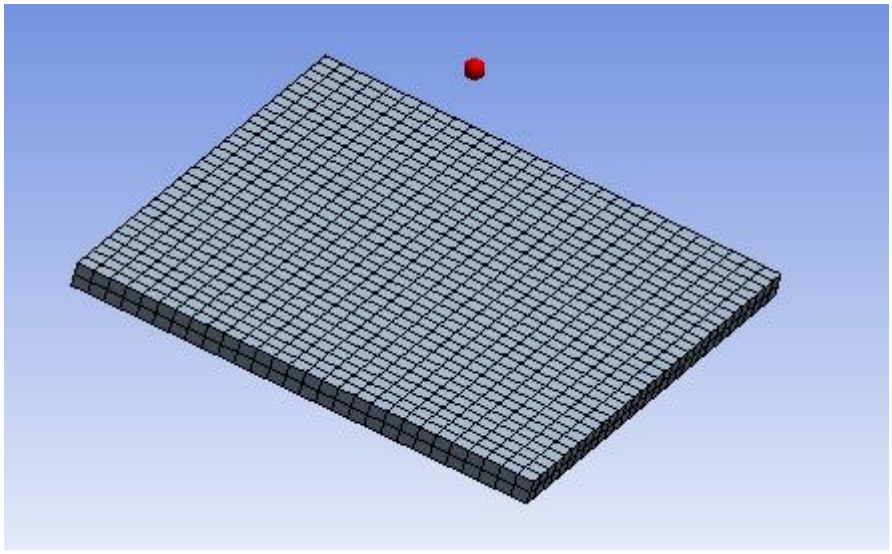

Fig 4-4 Base creation for gyroid lattice

Base creation for diamond lattice

Same base is created for diamond lattice structure as created before for the gyroid lattice structure.

4.2.4 Support structure generation

Majority of the selective laser melting processes require supports during the build process. ANSYS additive print module makes it very easy to generate support structures for the triply periodic minimal surface lattice structures. This module automatically generates supports for the lattice structures and so we don't need to separately design these supports and then add them to our lattice structures.

Support generation for gyroid lattice

Once the base of the gyroid lattice structure is created, its time to generate support structures for our gyroid lattice structure. ANSYS additive print module gives us the utility to automatically generate support structures for our gyroid lattice structure. So, support structures are automatically generated for gyroid lattice which is shown below:

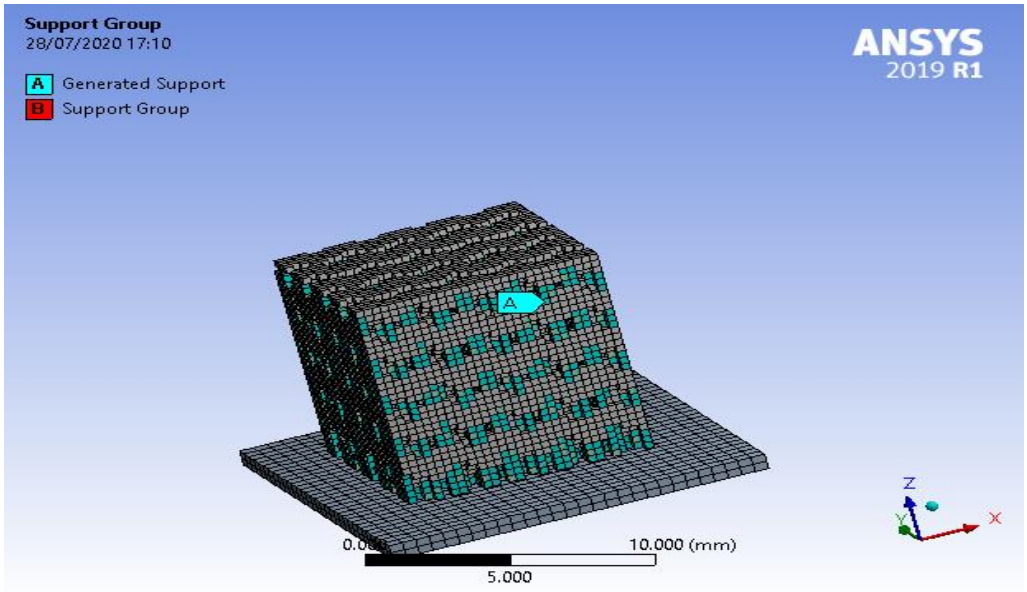

Fig 4-5 Supports generated for gyroid lattice

Support generation for diamond lattice

Similarly the support structures are automatically generated in case of diamond lattice structure. ANSYS additive print automatically detects and generates support structures for us so it makes very easy to generate support structures for our implant design. The supports generated for diamond lattice structure are shown below:

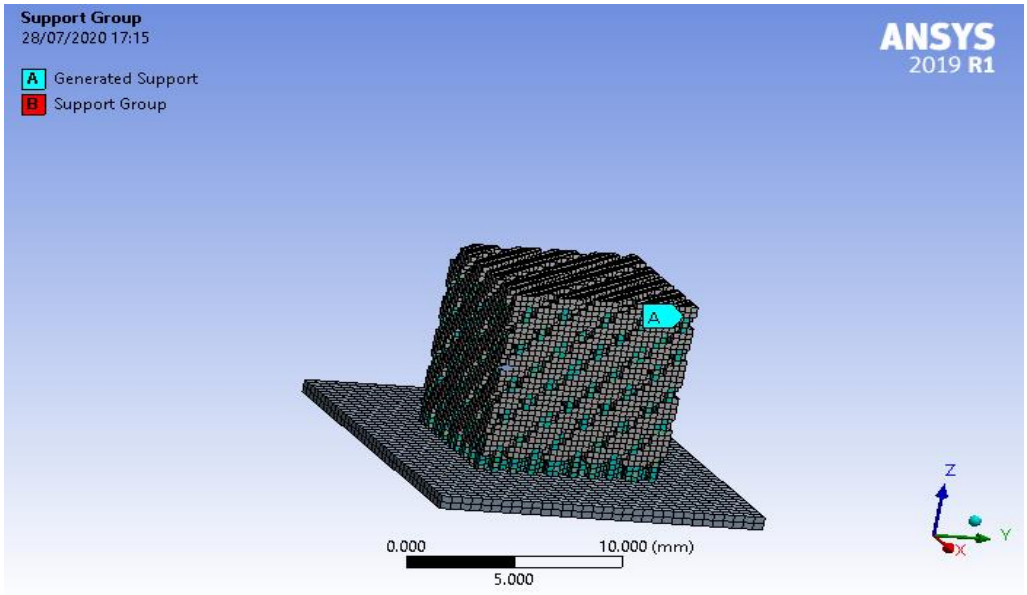

Fig 4-6 Supports generated for diamond lattice

4.2.5 Build settings for SLM process

The most important step in the selective laser melting process is the selection of optimum processing parameters so that we can get best results. These process parameters include layer thickness, scan speed and hatch spacing etc. These parameters directly affect the quality of the final parts. For example, if the scan speed is very low, then layers are exposed for more time and so the defect of over melting can occur. If the scan speed is very high, then the layers are exposed for less time and they get less amount of heat from the laser beam and so the layers are not properly melted which results in an inferior implant.

So, the optimum processing parameters should be used for best results. In this research work, we have used optimum process parameters for an ideal implant. Same processing parameters are used in the existing literature/research paper whose results will be compared and validated with our work in the next sections.

Build settings for Gyroid lattice

Build settings or processing parameters used for the gyroid lattice structure are shown below:

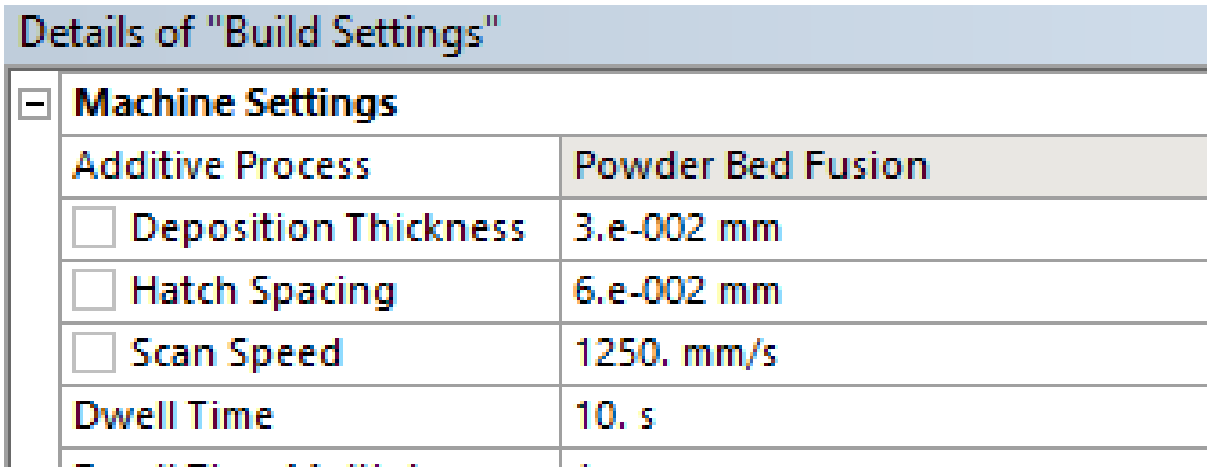

Fig 4-7 Build settings/processing parameters for gyroid lattice

Same processing parameters are used as used in the existing literature whom results we will compare and validate later with our work.

- Deposition thickness = 30µm
- Scan speed = 1250mm/s
- Hatch spacing = 60µm

Build settings for diamond lattice

Same build settings/process parameters are used for diamond lattice structure as were used previously in case of gyroid lattice structure.

4.2.6 Mesh generation

After performing the previous steps, mesh is generated for both the lattice structures i-e gyroid and diamond triply periodic minimal surface structures.

Gyroid lattice structure mesh generation

Mesh is generated for gyroid lattice structure as shown below:

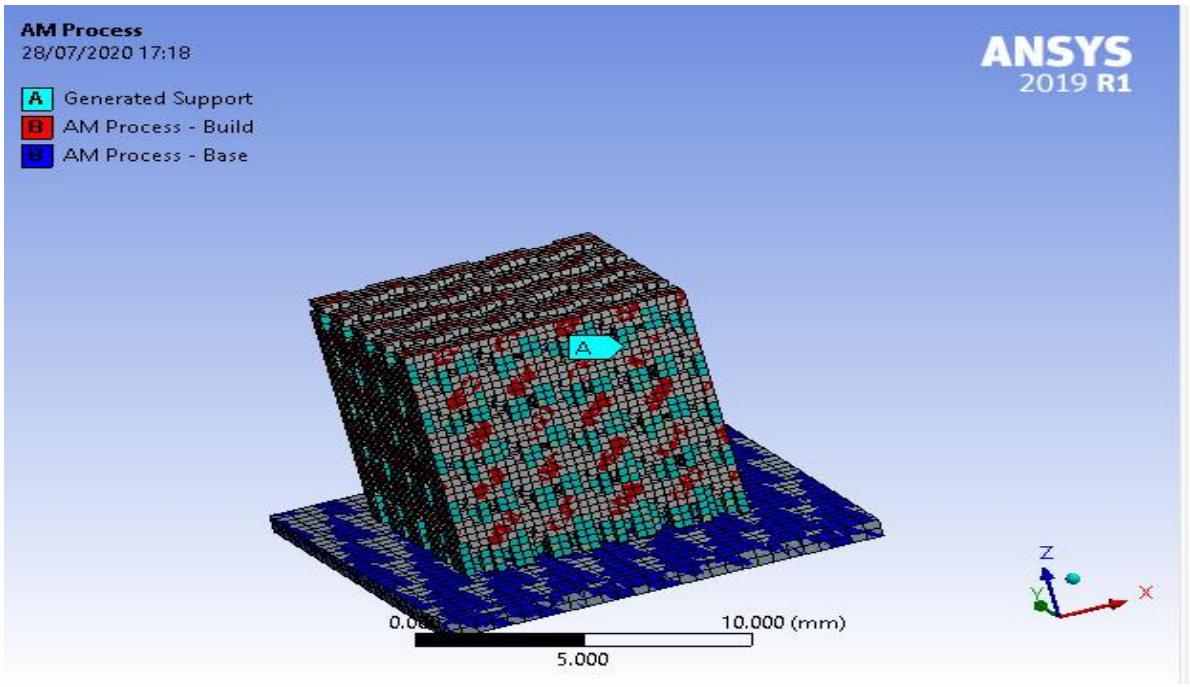

Fig 4-8 Gyroid lattice structure mesh generation

You can see in the above figure that:

- Red colour shows the part to be build
- Sky blue colour shows the generated support structures
- Blue colour shows the base

When the selective laser melting process is complete, the build part is separated and any needed post processing is done if required.

Diamond lattice structure mesh generation

Similarly mesh is generated for diamond lattice structure as was generated previously in case of gyroid lattice structure. Mesh generated is shown below:

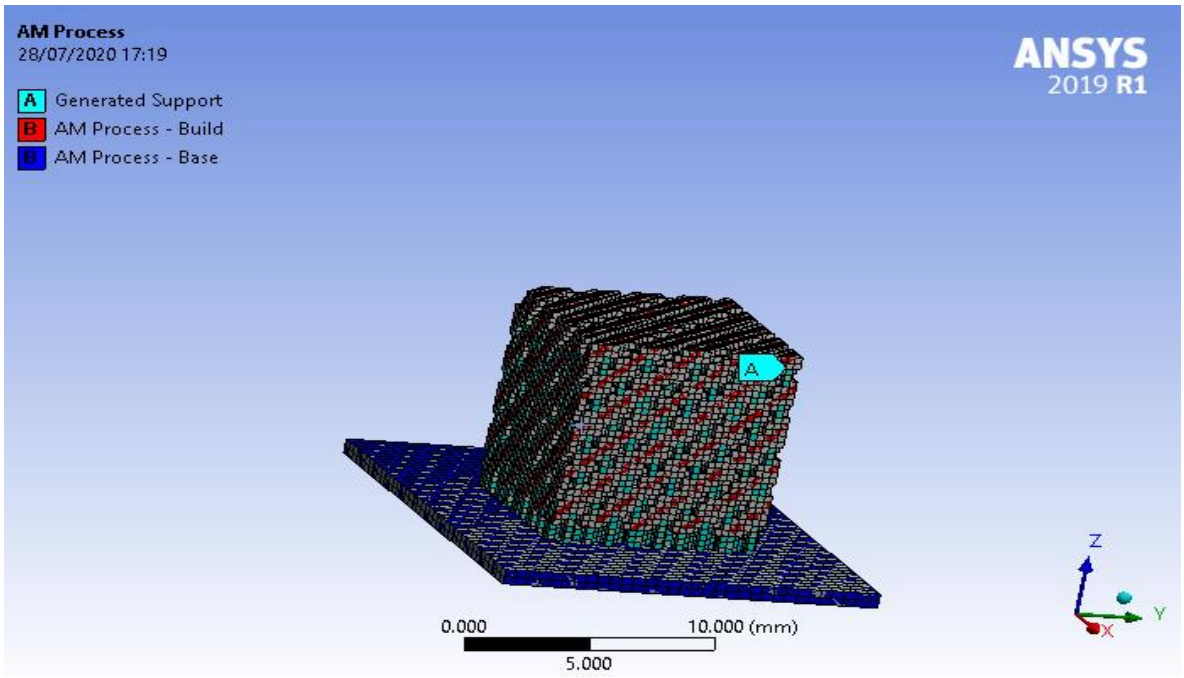

Fig 4-9 Diamond lattice structure mesh generation

An orthopaedic implant is inspected on the base of two mechanical properties:

- Modulus of elasticity
- Compression strength

An ideal implant should have a certain value ranges of modulus of elasticity and compression strength that are suitable for the human bone and it will be discussed in the next section. So, we will inspect our implant designs on the basis of these two mechanical properties which will be calculated and compared in the next section. We will also look for the manufacturability of our implant designs and will remove any problems during the build process if encountered.

4.2.7 Running the SLM process

After performing all the previous steps, we will now run the simulations of SLM process to get the final results. One thing must be noted that other ANSYS modules just import the part, perform static structural or thermal analysis and get the results but they do no offer us to model the complete build process and to monitor it. ANSYS additive print module gives us the utility

to model the whole selective laser melting process. It gives us the complete modelling control from importing the part to getting final results. It gives us results layer by layer and we can monitor the whole SLM process during the build process until the part is completed. If there are some problems occurred during the build, then it gives us full control to rectify these errors.

It gives us the insights of whole build process layer by layer and generates results with time after each layer is deposited till than the part is completed. It gives us the feel like if we are really manufacturing our part on the SLM machine and so this module is extremely useful for us and it is the first time ever this module of ANSYS is being used to model SLM process and no research work till date has been done which utilizes this new module.

The main concerns for the fabrication of orthopaedic implants were their manufacturability. It is reported in many research works, that the designed implant faces many manufacturability issues and some failures of its pores connections. This was a big headache for the designers of the orthopaedic implants because it was wasting a lot of money and time.

With the help of ANSYS additive print module, this problem is solved because using this software we can easily check the manufacturability of our implant and if some failures or problems are encountered during the manufacturability of the implants, then we can change our design or change the process parameters to rectify the problem without wasting our time and money. This is a new revolution in the field of orthopaedic implants and it has solved many problems.

After performing all the previous steps, we will now run our simulations and will get the results if no problem with manufacturability is occurred.

4.3 Calculations, results and validation

4.3.1 Manufacturability of the implants

In this section, manufacturability of the implants was inspected. Simulations of all the designed implants were run and no issue of manufacturability was encountered in any of the implant design. This indicates that our implant designs can be manufactured without any problems. So,

- All the implant designs meet the requirement of manufacturability.

4.3.2 Temperature distribution during the build process

As this module of ANSYS gives us the insights to the whole build process, we can easily monitor and get the temperature distribution during the whole build process. This is very useful because if there is excessive over melting at some stage of the build process or under melting, then we can easily monitor and look for the reason of this at a specific time of the build process

And we can rectify the problem by altering the build settings.

Temperature distribution for gyroid lattice structure

Temperature distribution of our first gyroid lattice implant design explained previously is as follows:

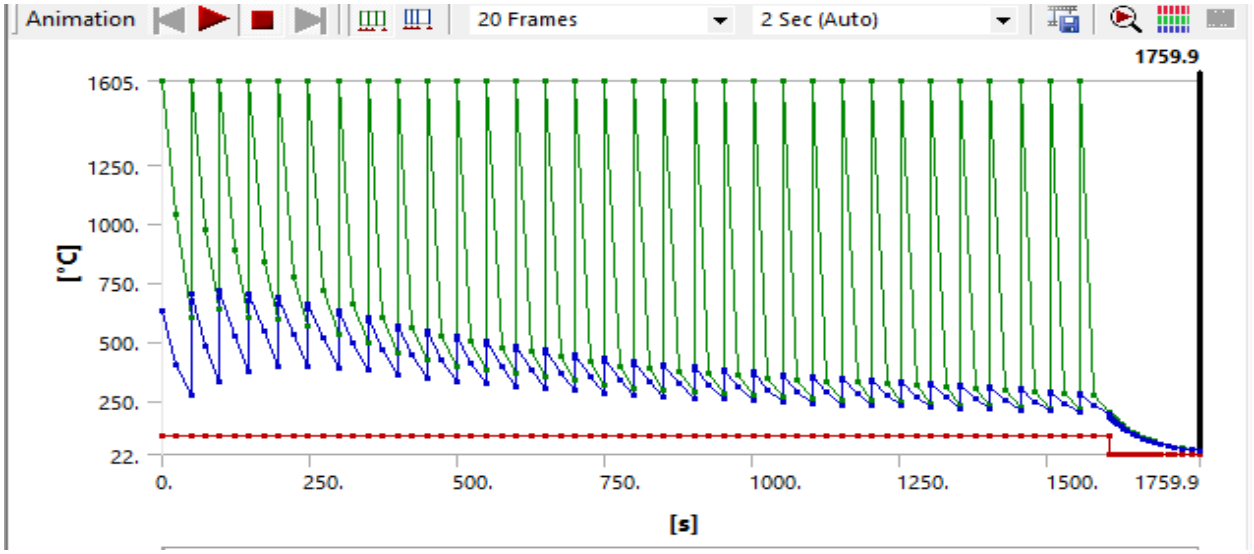

Fig 4-10 Gyroid lattice structure temperature distribution during build process

Temperature distribution for diamond lattice structure

Temperature distribution of our first diamond implant design explained previously is as follows:

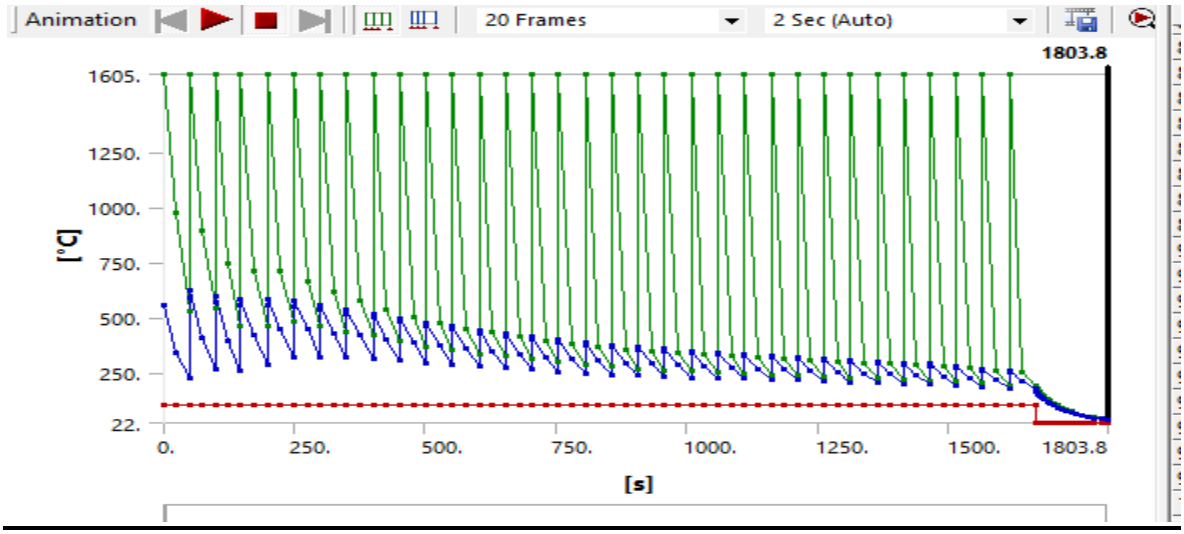

Fig 4-11 Diamond lattice structure temperature distribution during build process

4.3.3 Final manufactured part

We did not had the availability of the required SLM machine setup to physically manufacture our implant, but we can still get all the results during and after the build process of implant manufacturing using ANSYS additive print as if we were physically manufacturing our implant.

4.4.4 Elastic modulus calculations

This is the most important step for inspecting the quality of the orthopaedic implant. Human bone has very low modulus of elasticity as explained in the previous chapters. On the other hand, the modulus of elasticity of metals and alloys used for the implants are much higher as compared to the human bone. For example the modulus of elasticity of titanium alloy used in this research work is 110GPA which is much higher than that of the human bone. So, we designed gyroid and diamond TPMS lattice structures to lower the modulus of elasticity of the implant and to avoid the defect of stress shielding.

Now we will calculate the modulus of elasticity of our designed implant structures and will check whether they are suitable for the human bone or not. Gibson and Ashby provide relations between relative elastic modulus of solid and porous structures with the relative density of solid and porous structures. Their general form for TPMS structures is stated below:

$$\mathbf{E/E_S = C_1 (\rho/ \rho_S)^m}$$

Where, 'E_S'is the modulus of elasticity of solid material and 'E' is the modulus of elasticity of porous structure. 'ρ_S' is the density of solid material whereas 'ρ' is the density of porous structure. Value of 'C_1' Coefficient ranges between 0.1-4.0. Value of 'm' is approximately equal to '2'.

For gyroid and diamond TPMS structures, this equation is modified as follows:

Gyroid Relation

$$\mathbf{E/E_S = 0.19(\rho/ \rho_S)^{1.71}}$$

Diamond relation

$$\mathbf{E/E_S = 0.17(\rho/ \rho_S)^{1.64}}$$

Where 'E_S'is the modulus of elasticity of solid material and 'E' is the modulus of elasticity of porous structure. 'ρ_S' is the density of solid material whereas 'ρ' is the density of porous structure.

By using the above relations we can easily calculate the modulus of elasticity of our implant designs. Modulus of elasticity for solid material 'E_S'is 110GPA and we also know that the density of the solid material 'ρ_S' is 4.405e-6 Kg mm^{-3} . We just need to know the density of the porous structure and we can easily get the modulus of elasticity of our porous implant structure.

We know that:

Density = mass/volume

We just need to know the final volume of porous implant and the mass of the porous implant and we will get the density of the porous implant.

ANSYS additive print module makes it very easy for us as it gives us the final volume and mass of the porous metallic implant and we can easily calculate the density of the porous implant.

Modulus of elasticity of Gyroid structure

To calculate the modulus of elasticity of gyroid structure, we first need to know the density of the porous gyroid implant structure. We have already done the complete simulations of selective laser melting process and by using ANSYS additive print module, we can easily get the final volume and mass of the gyroid lattice structure. So, the density of our first porous implant design is as follows:

ρ= (7.4632e-004)/(428.44)

ρ= 1.741947531e-6 kg mm^{-3}

Now we will put the value of porous implant density in the main relation of the gyroid lattice.

$$\mathbf{E/E_S = 0.19(\rho/\ \rho_S)^{1.71}}$$

$E/\ 110 = 0.19((1.741947531E\text{-}6)/(4.405E\text{-}6))^{1.71}$

$E/\ 110 = 0.03888445883$

E = 4.277GPA

So, the modulus of elasticity of our first porous gyroid implant design is 4.277GPA which is completely compatible with the human trabecular bone. It has reduced from 110GPA to 4.277GPA. Human trabecular bone has modulus of elasticity equal to 1.08 $\pm$0.86 GPA. It can go to a maximum of 8GPA. Our first implant design has modulus of elasticity ideal for trabecular bone hence it meets the requirements of trabecular bone and so this implant can be physically used in the human body because it is fully compatible with the human body and also has the appropriate pore size for cells and tissues ingrowths.

TPMS designs have proved to be the best designs for the orthopaedic implants due to which the modulus of elasticity has fallen from 110 to 4.277GPA and the implant is fully compatible with the human body and the all time big concern of stress shielding is also avoided.

Modulus of elasticity of diamond structure

By following the similar procedure as adopted in the case of gyroid lattice structures, we can get the density of porous structure as follows:

ρ= (6.3503e-004)/(466.4)

ρ= 1.361556604e-6 kg mm^{-3}

Putting the density of the porous structure in the main relation of the diamond lattice structure:

$$\mathbf{E/E_S = 0.17(\rho/\rho_S)^{1.64}}$$

$E/110 = 0.17((1.361556604e\text{-}6)/(4.405e\text{-}6))^{1.64}$

E/110 = 0.02478541381

E = 2.726GPA

The modulus of elasticity of the diamond porous implant structure is 2.726GPA. It has reduced from 110GPA to 2.726GPA. It has elastic modulus ideal for the human trabecular bone and also has the appropriate pore size needed for cells and tissues ingrowths. It is fully compatible with the human body and it can be physically installed in the body as bone implant.

4.4.5 Other gyroid and diamond implant designs

All the implants designed in this research work follow the same steps as explained previously. The results of all the implant designs are shown below in the table:

S. no	Type	Pore size (μm)	Porosity %	Elastic modulus 'E' GPA	Density Kg mm^{-3}
1	Gyroid	1220	60.45	4.277	1.741947531e-6
2	Diamond	1160	69.08	2.726	1.361556604e-6
3	Gyroid	780	70.49	2.591	1.29938882e-6
4	Diamond	740	79.49	1.391	9.033992702e-7
5	Gyroid	620	76.03	1.816	1.055734106e-6
6	Diamond	570	80.02	1.332	8.799064436e-7
7	Gyroid	440	76.75	1.723	1.02377778e-6
8	Diamond	400	84.64	0.865	6.764444444e-7

Table 4-1 Different orthopaedic implant designs and results

All the implants designed in this research work meet the requirements of human trabecular bone and also they have no issues related with the manufacturability. They also have the appropriate pore sizes for cells and tissues ingrowths. So, all the implants designed in this research work can be physically used in the human body because they meet all the requirements for bone implants.

4.4.6 Calculation of compression strength

Using Gibson and Ashby relations, we can easily calculate compression strengths of our designed implants.

Compression strength for gyroid structure

Compression strength of gyroid lattice can be calculated using following relation:

$$\mathbf{E = 24.05\ (\sigma_{max})^{0.90}}$$

Where 'E' is the modulus of elasticity of the porous implant in MPA, σ_{max} is the compression strength in MPA

We can easily calculate compression strength for all implant designs.

Compression strength for diamond structure

Compression strength of diamond lattice can be calculated using following relation.

$$\mathbf{E = 30.92(\sigma_{max})^{0.88}}$$

Where 'E' is the modulus of elasticity of the porous implant in MPA, σ_{max} is the compression strength in MPA

We can easily calculate compression strength for all implant designs.

The table below shows the compression strengths of different implant designs:

S.no	Type	Elastic modulus (MPA)	Compression strength (MPA)
1	Gyroid	4277	316.247
2	Gyroid	2591	181.204
3	Gyroid	1816	122.086
4	Gyroid	1723	115.159
5	Diamond	2726	162.387
6	Diamond	1391	75.597
7	Diamond	1332	71.964
8	Diamond	865	44.062

Table 4-2 Compression strengths of different implant designs

The compression strengths of all the implant designs also meet the requirements of the human bone so ideal orthopaedic implants with different designs are created in this research work and can be physically installed in the human body and these implants are fully compatible with the human body.

4.4.7 Yield strength relations

Gibson and Ashby also provide relations between relative density and relative yield strength.

Gyroid Relations

The relation between relative density and relative yield strength modified for gyroid lattice structure is shown below:

$$\sigma/\sigma_s = 1.31(\rho/\rho_S)^{1.83}$$

Where 'σ_s' is the yield strength of fully dense solid and its value is 1.24GPA. Value of 'σ'can be calculated easily as we know the relative density for each design.

Diamond relation

The relation between relative density and relative yield strength modified for diamond lattice structure is shown below:

$$\sigma/\sigma_s = 1.39(\rho/\rho_S)^{1.95}$$

Where 'σ_s' is the yield strength of fully dense solid and its value is 1.24GPA. Value of 'σ'can be calculated easily as we know the relative density for each design.

The graphical results of yield strength relations are shown in the next section.

4.5 Validation of the results with existing literature

All the implant design results were compared and validated with the existing literature. The following table shows the comparison of our implant design results with the existing literature/research paper:

Gyroid literature and diamond literature shows the results of the existing literature/research paper whose results we will compare and validate with our work whereas, gyroid and diamond type shows the results of our implant designs that are developed in this research work.

S. no	Type	Pore size µm	Porosity %	Elastic modulus (GPA)	Compression strength (MPA)
1	Gyroid literature	560-1600	80-95	0.13-1.25	8.12-83.9
2	Diamond literature	480-1450	80-95	0.12-1.25	6.79-73.43
3	Gyroid	440-1220	60.45-76.75	1.732-4.277	115.15-316.24
4	Diamond	400-1160	69.08-84.64	0.865-2.726	44.06-162.38
5	Trabecular bone	-	50-90	1.08 ±0.86GPA	-

Table 4-3 Comparison and Validation of our implant designs with existing literature

The implants designed and manufactured in the existing literature/research paper have a porosity range of 80-95% whereas in our research work, the porosity ranges are between 50-90% that is the required porosity range for trabecular bone. Moreover, the pore size and design in our research work is also slightly different from the existing literature. The reason for changing the implant designs were to obtain implants that are ideal for the human body and so the porosity range was selected between the range of trabecular bone and also the pore sizes that will result in maximum cells and tissues ingrowths were selected in our design. Due to these design differences, our results are slightly different when we compare it with existing literature but the results follow the same trends as followed by the existing literature/research work. Compression strengths also change by a huge amount when a slight change in implant design is done.

All of our implant designs meet the requirements of the human bone and their results also follow the same trends as followed in the existing literature/research paper and so our results are also validated with the existing literature with slight variations in the results due to the design change of the implants as discussed previously.

So, in the end, all of the implants designed in this research work are biocompatible, have no manufacturability issues, have suitable mechanical properties required for human bone and in short they meet all the necessary requirements for the ideal implants and can be physically installed in the human body as they are fully compatible with the human body.

4.6 Graphical representations

In this section, graphical representations of the results will be presented.

4.6.1 Elastic modulus vs. porosity

According to the existing literature, we know that porosity has inverse relationship with the modulus of elasticity. If a structure is less porous, its modulus of elasticity will be greater. On the other hand, if a structure is highly porous, its modulus of elasticity will be very low. The graphical representation below shows the relationship between porosity and elastic modulus

based on our results of the designed implants in this research work.

Gyroid lattice structure

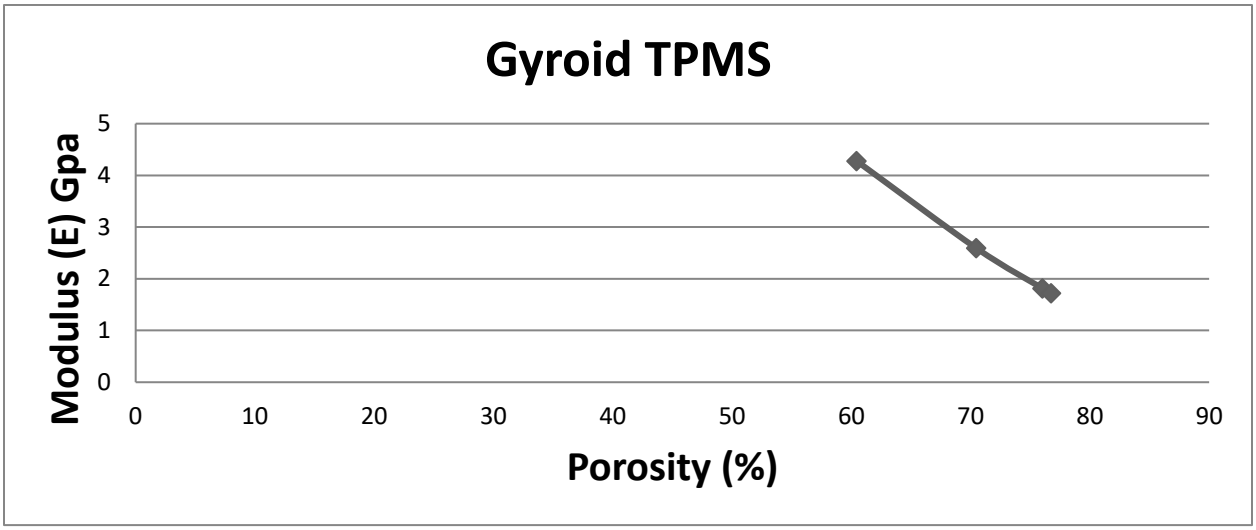

Fig 4-12 Gyroid structure Elastic modulus vs. porosity graph

From our results, we can see that porosity and elastic modulus have inverse relationship and by increasing porosity levels, Elastic modulus is decreasing. So, our results follow the same trends as followed by existing literature, so our work is validated.

Diamond lattice structure

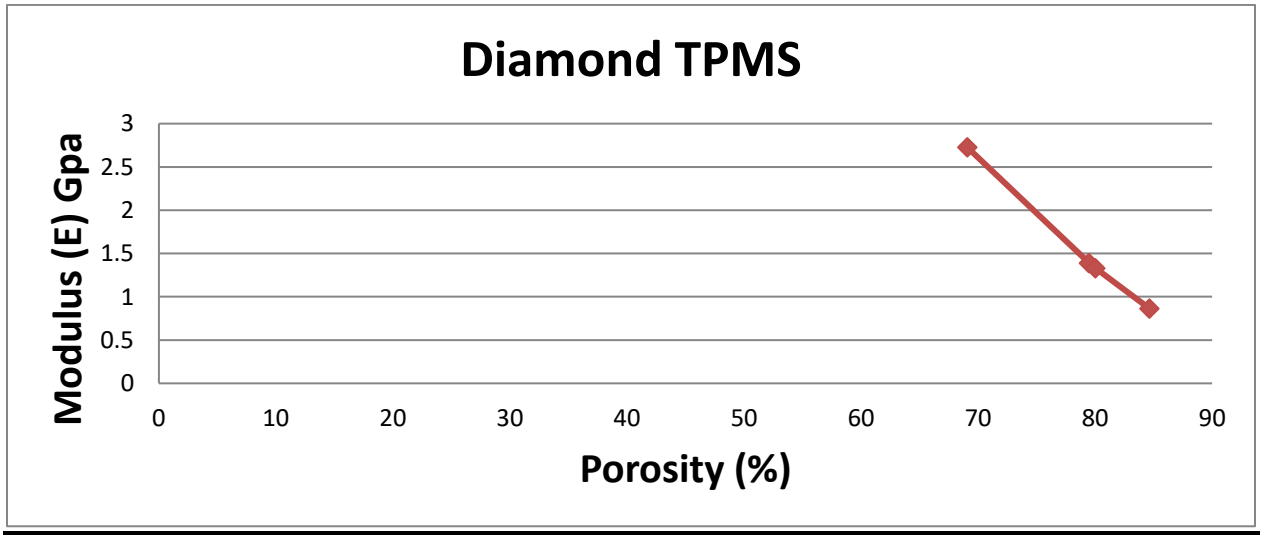

Fig 4-13 Diamond structure Elastic modulus vs. porosity graph

From our results, we can see that porosity and elastic modulus have inverse relationship and by increasing porosity levels, Elastic modulus is decreasing. So, our results follow the same trends as followed by existing literature, so our work is validated.

4.6.2 Elastic modulus vs. pore size

According to the existing literature, pore size and elastic modulus are directly proportional. If the structure has larger pores, it has less porosity and so its modulus of elasticity will be greater. Similarly, if a structure has small size pores, then the structure is more porous and so the modulus of elasticity will be less.

Gyroid lattice structure

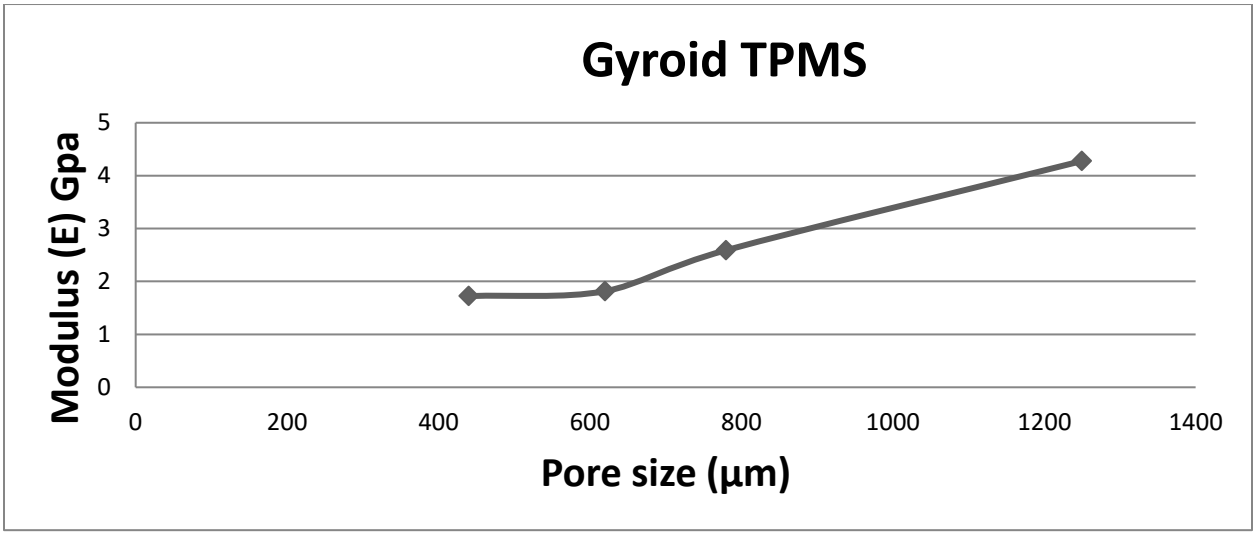

Fig 4-14 Gyroid structure elastic modulus vs. pore size

In the above graph, we can see that value of elastic modulus increases with the increase in pore size and it follows the same rends as followed by existing literature, and so our work is validated.

Diamond lattice structure

Elastic modulus vs. pore size graph in case of diamond lattice structure is presented in the next page.

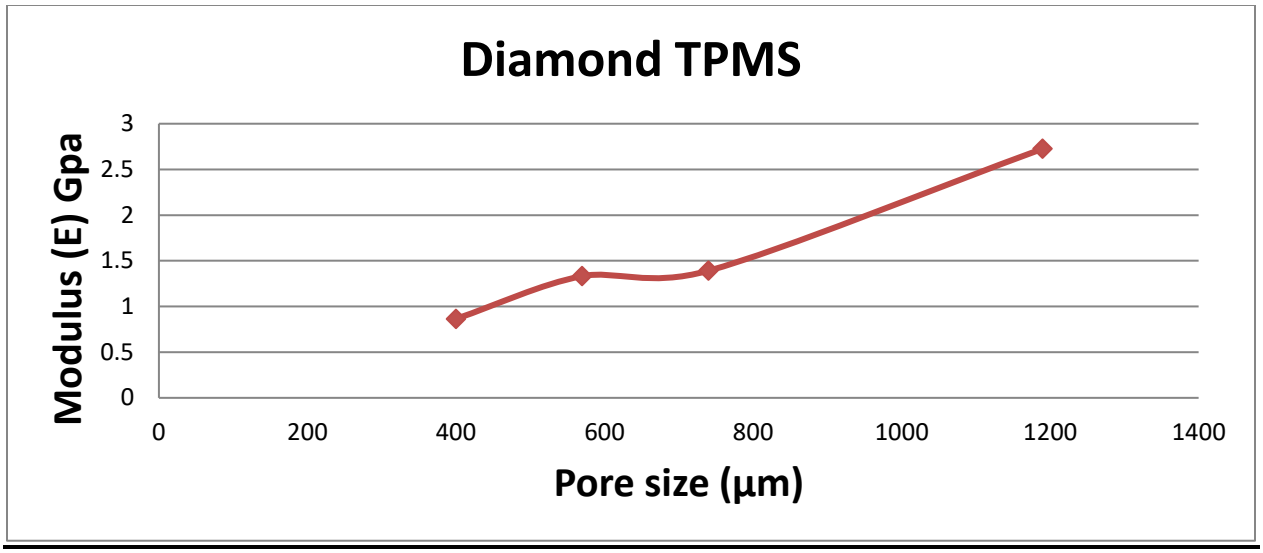

Fig 4-15 Diamond structure elastic modulus vs. pore size

In the above graph, we can see that value of elastic modulus increases with the increase in pore size and it follows the same rends as followed by existing literature, and so our work is validated.

4.6.3 Relative density vs. Relative modulus

Gyroid lattice structure

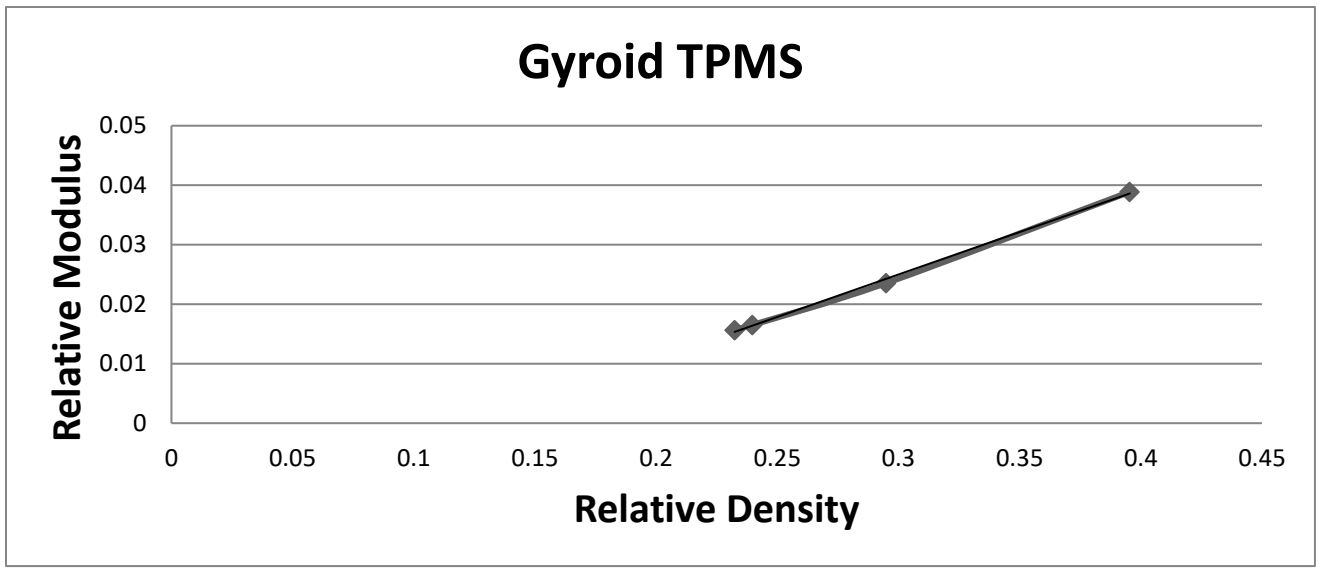

Fig 4-16 Gyroid Relative density vs. Relative modulus graph

Diamond lattice structure

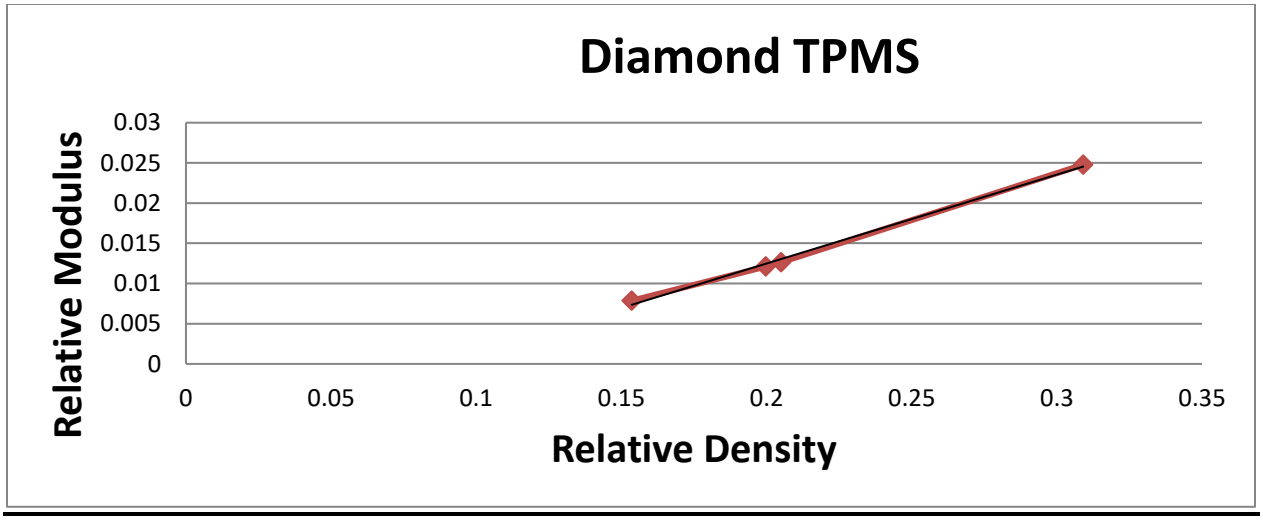

Fig 4-17 Diamond Relative density vs. Relative modulus graph

4.6.4 Compression strength vs. Elastic modulus

Gyroid porous structure

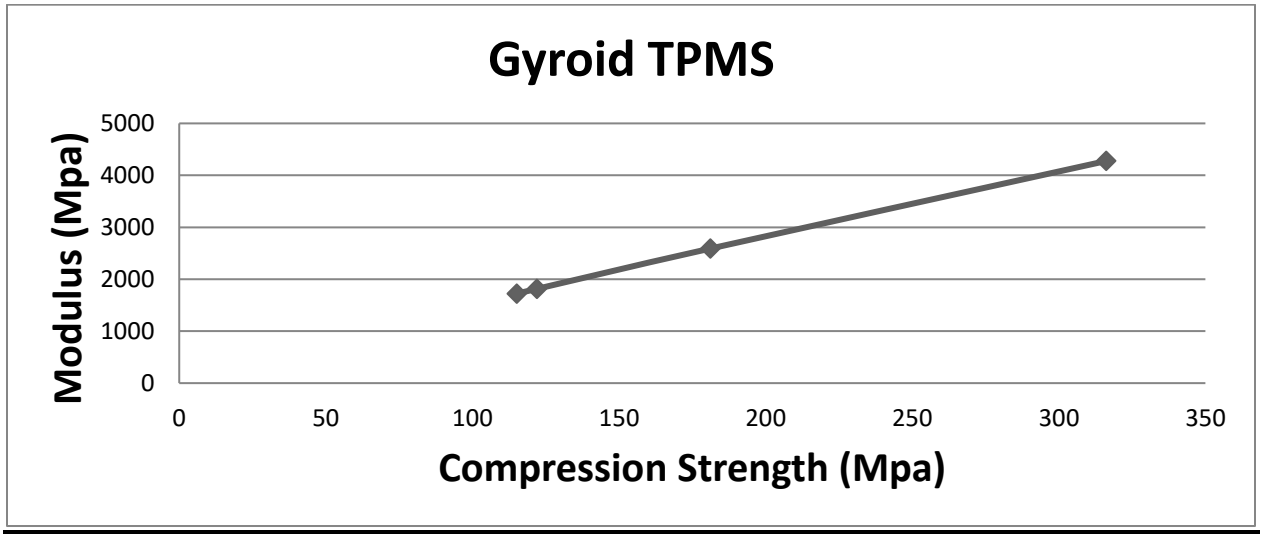

Fig 4-18 Gyroid compression strength vs. Elastic modulus graph

Diamond porous structure

The relationship between compression strength and elastic modulus in case of diamond porous lattice structure is presented in the graph below:

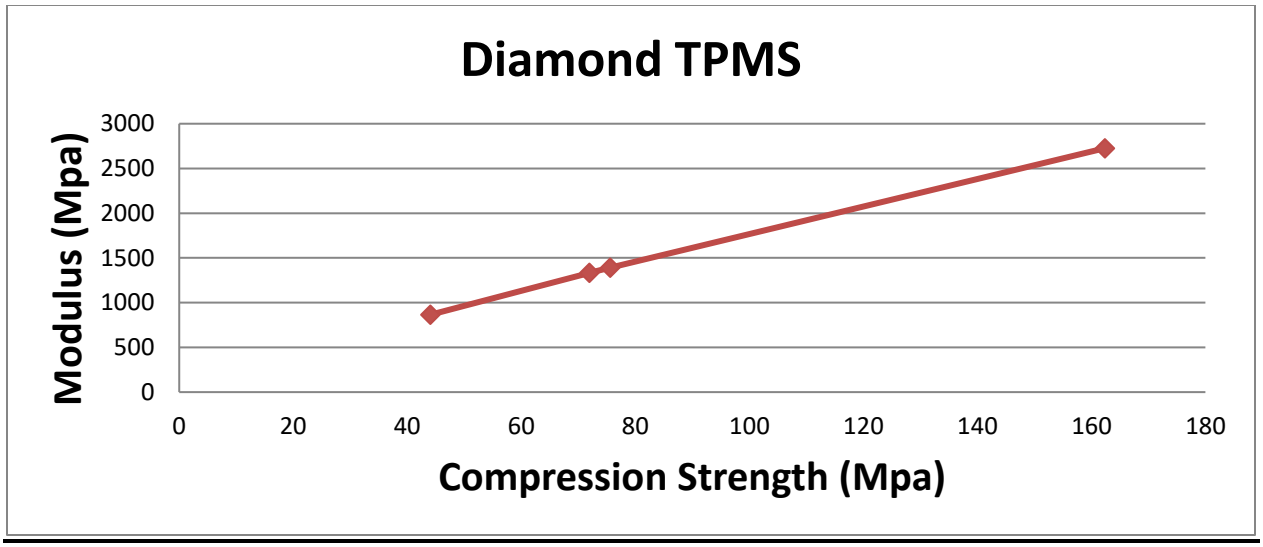

Fig 4-19 Diamond compression strength vs. Elastic modulus graph

4.6.5 Relative density vs. Relative strength

Gyroid TPMS

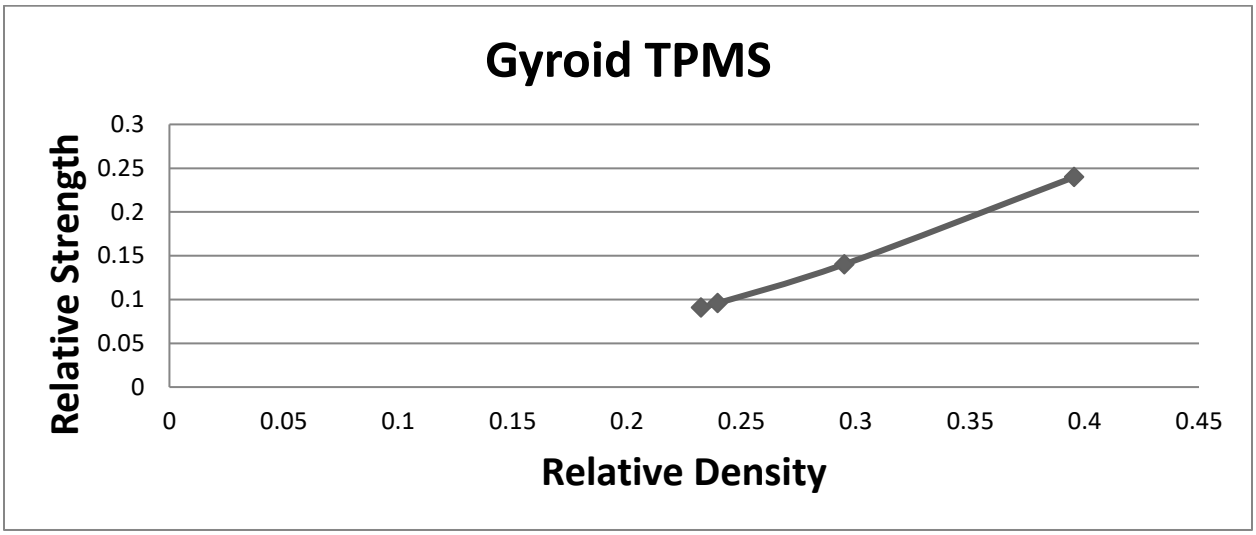

Fig 4-20 Gyroid Relative density vs. Relative strength graph

Diamond TPMS

The relationship between relative density and relative strength in case of diamond TPMS lattice structure is presented below in the graph.

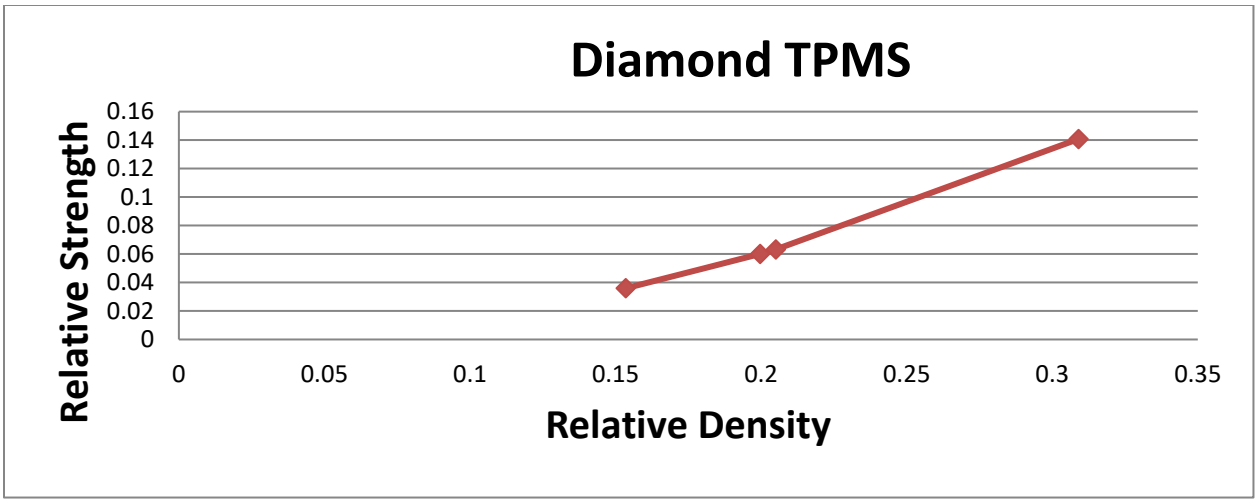

Fig 4-21 Diamond Relative density vs. Relative strength graph

All of our results follow the same trends as followed in the existing literature and our work is validated.

4.7 Combined graphs for comparisons and validations of results

The combined graph showing the relationship between relative density and relative modulus and comparison and validation of our results with the results of existing literature/research paper is shown below:

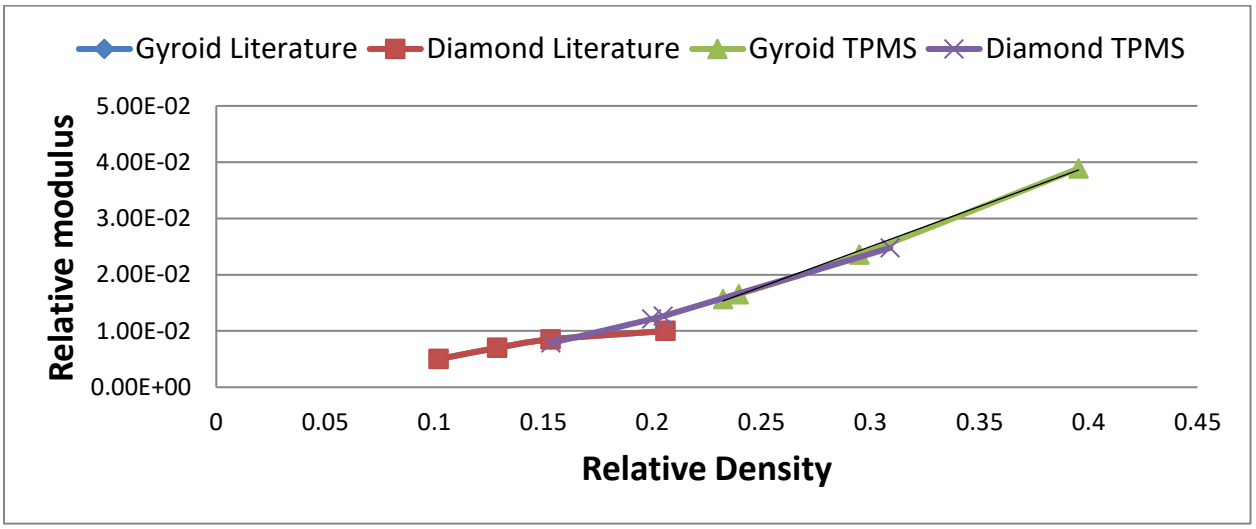

Fig 4-22 Validation of our results with existing literature/research paper

From the above results, it is concluded that our implant design results follow the same trends as followed by the existing literature/research paper and so our research work is validated with the existing literature/research paper. There are very slight variations in the final results and it is because our designs were little different from the designs of the existing literature/research paper.

Relative density vs. relative strength combined graph

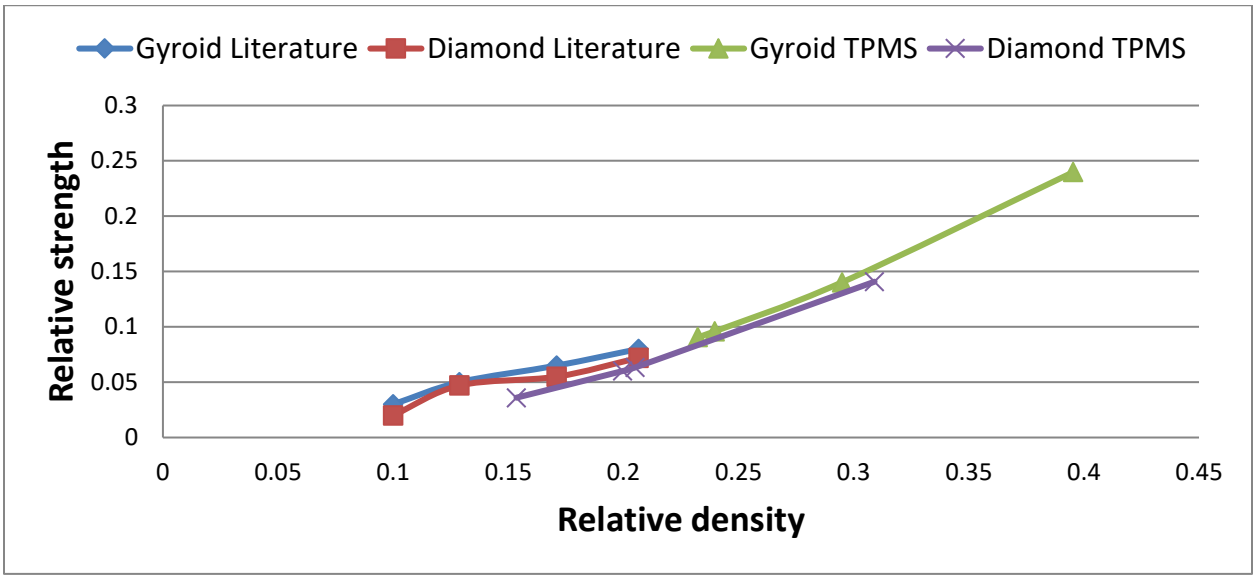

Fig 4-23 Relative density vs. Relative strength combined graph results validations

From the above results, it is concluded that our implant design results follow the same trends as followed by the existing literature/research paper and so our research work is validated with the existing literature/research paper. There are very slight variations in the final results and it is because our designs were little different from the designs of the existing literature/research paper.

Conclusions and future recommendations are presented in the next chapter.

Chapter #5

Conclusions and future Recommendations

Orthopaedic implants are considered to be very vital in the medical industry. They have proved to be very useful in the human body. However, these implants were causing many problems once they were installed in the human body. The biggest concern for the implant manufacturers was stress shielding which was very damaging for the human body. This was caused due to a large mismatch between the modulus of elasticity of the implant and the modulus of elasticity of the human bone. The materials used for the manufacturing of orthopaedic implants had a very high modulus of elasticity as compared to the human bone, so there was a need to lower that modulus of elasticity to the levels close to the human bone and so they become suitable for the human body.

In this research work, we focussed on this problem and introduced gyroid and diamond TPMS structures, designed different models of the implants and removed the problem of stress shielding. For the first time ever, we used a new module of ANSYS known as ANSYS additive module which can model the whole selective laser melting process and can also check the manufacturability of the implants. No research work was done till date, which made use of ANSYS additive print module. So, for the first time ever, we used this module to model whole selective laser melting process.

Different implant designs were created in this research work and all of them meet the requirements of an ideal implant and so can be physically installed in the human body without facing any problems as these implants are fully compatible with the human body. No problems related with the manufacturability were encountered. In the end, all the results were compared and validated with the existing literature/research paper. The bone implant designs modelled in this research work can be physically manufactured as an future recommendation.

In future, new TPMS structures can be discovered and designed for the medical orthopaedic implants. Majority of the implants make use of titanium alloy due to its good biocompatibility and good mechanical properties, In future, new alloys can be discovered which have the desired properties needed for an orthopaedic implant. Research works are recommended in this field for future recommendations.

References

1. Additive Manufacturing Technologies 3D Printing, Rapid Prototyping, and Direct Digital Manufacturing (Ian Gibson et al., 2010).

2. A review of additive manufacturing technologies https://www.researchgate.net/publication/322745252
3. Review of selective laser melting: Materials and applications, C. Y. Yap, C. K. Chua, Z. L. Dong, Z. H. Liu, D. Q. Zhang, L. E. Loh, and S. L. Sing, http://dx.doi.org/10.1063/1.4935926
4. N. K. Tolochko, Y. V. Khlopkov, S. E. Mozzharov, M. B. Ignatiev, T. Laoui, and V. I. Titov, Rapid Prototyping J. 6, 155–161 (2000).

5. P. Fischer, V. Romano, H. P. Weber, N. P. Karapatis, E. Boillat, and R. Glardon, Acta Mater. 51, 1651–1662 (2003).
6. A. V. Gusarov and J. P. Kruth, Int. J. Heat Mass Transfer 48, 3423–3434 (2005).
7. L. E. Loh, Z. H. Liu, D. Q. Zhang, M. Mapar, S. L. Sing, C. K. Chua, and W. Y. Yeong, Virtual Phys. Prototyping 9, 11–16 (2014).
8. . K. Mumtaz and N. Hopkinson, Rapid Prototyping J. 16, 248–257 (2010).
9. D. Bourell, A. B. Spierings, N. Herres, and G. Levy, Rapid Prototyping J. 17, 195–202 (2011).
10. B. Liu, R. Wildman, C. Tuck, I. Ashcroft, and R. Hague, in International Solid Freeform Fabrication Symposium: An Additive Manufacturing Conference (University of Texas at Austin, Austin, 2011), pp. 227–238.
11. N. K. Tolochko, S. E. Mozzharov, I. A. Yadroitsev, T. Laoui, L. Froyen, V. I. Titov, and M. B. Ignatiev, Rapid Prototyping J. 10, 78–87 (2004).
12. R. Li, J. Liu, Y. Shi, L. Wang, and W. Jiang, Int. J. Adv. Manuf. Technol. 59, 1025–1035 (2011).
13. J. P. Kruth, L. Froyen, J. Van Vaerenbergh, P. Mercelis, M. Rombouts, and B. Lauwers, J. Mater. Process. Technol. 149, 616–622 (2004).
14. Review on manufacture by selective laser melting and properties of titanium based materials for biomedical applications for biomedical applications, DOI:10.1179/1753555715Y.0000000076
15. Processing parameters for selective laser sintering or melting of oxide ceramics by haidong zhang and Saniya LeBlanc DOI: 10.5772/intechopen.75832
16. Applications of the Selective Laser Melting Technology in the Industrial and Medical Fields By Pacurar Razvan and Pacurar Ancuta Submitted: October 19th 2015 Reviewed: March 11th 2016 Published: July 13th 2016 DOI: 10.5772/63038
17. Additive manufacturing technology for porous metal implant applications and triple minimal surface structures: A review Li Yuan, Songlin Ding**, Cuie Wen* School of Engineering, RMIT University, Bundoora, Victoria, 3083, Australia http://www.keaipublishing.com/biomat

18. . E.B. Goudie, C. Robinson, P. Walmsley, I. Brenkel, Changing trends in total knee replacement, Eur. J. Orthop. Surg. Traumatol. 27 (2017) 539–544 http://doi.org/10.1007/s00590-017-1934-8.
19. E. Losina, J.N. Katz, Total knee arthroplasty on the rise in younger patients: are we sure that past performance will guarantee future success, Arthritis Rheum. 64 (2012) 339–341 http://doi.org/10.1002/art.33371.
20. K. Prasad, O. Bazaka, M. Chua, M. Rochford, L. Fedrick, J. Spoor, R. Symes, M. Tieppo, C. Collins, A. Cao, D. Markwell, K. Ostrikov, K. Bazaka, Metallic biomaterials: current challenges and opportunities, Materials 10 (2017) 884 https://doi.org/10.3390/ma10080884.
21. L.C. Palmer, C.J. Newcomb, S.R. Kaltz, E.D. Spoerke, S.I. Stupp, Biomimetic systems for hydroxyapatite mineralization inspired by bone and enamel, Chem. Rev. 108 (2008) 4754–4783 https://pubs.acs.org/doi/abs/10.1021/cr8004422.
22. Ti based biomaterials, the ultimate choice for orthopaedic implants – A review M. Geetha a,*, A.K. Singh b, R. Asokamani a, A.K. Gogia c z www.elsevier.com/locate/pmat sci
23. Additive manufacturing technology for porous metal implant applications and triple minimal surface structures: A review Li Yuan, Songlin Ding**, Cuie Wen* School of Engineering, RMIT University, Bundoora, Victoria, 3083, Australia http://www.keaipublishing.com/biomat
24. Science Learning Hub, Toxicity, (2009) https://www.sciencelearn.org.nz/resources/1540-toxicity , Accessed date: 9 June 2018.
25. Department of health, What You Know Can Help You - an Introduction to Toxic Substances, (2013) https://www.health.ny.gov/environmental/chemicals/toxic_substances.htm , Accessed date: 8 June 2018.
26. M. Jaishankar, T. Tseten, N. Anbalagan, B.B. Mathew, K.N. Beeregowda, Toxicity, mechanism and health effects of some heavy metals, Interdiscipl. Toxicol. 7 (2014) 60–72 https://doi.org/10.2478/intox-2014-0009.
27. Q. Chen, G.A. Thouas, Metallic implant biomaterials, Mater. Sci. Eng. R Rep. 87 (2015) 1–57 https://doi.org/10.1016/j.mser.2014.10.001.
28. L.M. Plum, L. Rink, H. Haase, The essential toxin: impact of zinc on human health, Int. J. Environ. Res. Publ. Health 7 (2010) 1342–1365 https://doi.org/10.3390/ijerph7041342.
29. K.S. Egorova, V.P. Ananikov, Toxicity of metal compounds: knowledge and myths, Organometallics 36 (2017) 4071–4090 https://pubs.acs.org/doi/full/10.1021/acs.organomet.7b00605.
30. D.F. Williams, There is no such thing as a biocompatible material, Biomaterials 35 (2014) 10009–10014 https://doi.org/10.1016/j.biomaterials.2014.08.035.
31. F.J. O'Brien, Biomaterials & scaffolds for tissue engineering, Mater. Today 14 (2011) 88–95 https://doi.org/10.1016/S1369-7021(11)70058-X
32. N. Little, B. Rogers, M. Flannery, Bone formation, remodeling and healing, Surgery 29 (2011) 141–145 https://doi.org/10.1016/j.mpsur.2011.01.002.
33. C.S. Terrier, P. Gasque, Bone responses in health and infectious diseases: a focus on osteoblasts, J. Infect. 75 (2017) 281–292 https://doi.org/10.1016/j.jinf.2017.07.007.

34. K.L. Bundy, Biomaterials and the Chemical Environment of the Body, Joint Replacement Technology, (2008), pp. 56–80 https://doi.org/10.1533/9781845694807.1.56.
35. L.A.G. Armas, J.M. Lappe, R.P. Heaney, Chapter 19 - calcium, bone strength and fractures, Osteopor. Men (2010) 235–241 https://doi.org/10.1016/B978-0-12-374602-3.00019-5.
36. A. Biesiekierski, J. Wang, M.A. Gepreel, C. Wen, A new look at biomedical Tibased shape memory alloys, Acta Biomater. 8 (2012) 1661–1669 https://doi.org/10.1016/j.actbio.2012.01.018.
37. A. Ataee, Y. Li, D. Fraser, G. Song, C. Wen, Anisotropic Ti-6Al-4V gyroid scaffolds manufactured by electron beam melting (EBM) for bone implant applications, Mater. Des. 137 (2018) 345–354 https://doi.org/10.1016/j.matdes.2017.10.040.
38. The microstructural and biomechanical development of the condylar bone: A review DOI: 10.1093/ejo/cjt093
39. Sevilla, P., Aparicio, C., Planell, J.A., Gil, F.J., 2007. Comparison of the mechanical properties between tantalum and nickel- titanium foams implant materials for bone in growth applications. J. Alloy. Compd. 439, 67–73.
40. G. Poumarat, P. Squire, Comparison of mechanical properties of human, bovine bone and a new processed bone xenograft, Biomaterials 14 (1993) 337–340 https://doi.org/10.1016/0142-9612(93)90051-3.
41. Additive manufacturing technology for porous metal implant applications and triple minimal surface structures: A review Li Yuan, Songlin Ding**, Cuie Wen* School of Engineering, RMIT University, Bundoora, Victoria, 3083, Australia http://www.keaipublishing.com/biomat
42. Characteristics of Metals Used in Implants, DOI: 10.1089/end.1997.11.383
43. M. Moravej, D. Mantovani, Biodegradable metals for cardiovascular stent application: interests and new opportunities, Int. J. Mol. Sci. 12 (2011) 4250–4270
44. P. Wen, L. Jauer, M. Voshage, Y. Chen, R. Poprawe, J.H. Schleifenbaum, Densification behavior of pure Zn metal parts produced by selective laser melting for manufacturing biodegradable implants, J. Mater. Process. Technol. 258 (2018) 128–137 https://doi.org/10.1016/j.jmatprotec.2018.03.007
45. A. Carlos, Leon y Leon, New perspectives in mercury porosimetry, Adv. Colloid Interface Sci. 76–77 (1998) 341–372.
46. A. Yánez, A. Cuadrado, O. Martel, H. Afonso, D. Monopoli, Gyroid porous titanium structures: a versatile solution to be used as scaffolds in bone defect reconstruction, Mater. Des. 140 (2018) 21–29 https://doi.org/10.1016/j.matdes.2017.11.050.
47. V. Karageorgiou, D. Kaplan, Porosity of 3D biomaterial scaffolds and osteogenesis, Biomaterials 26 (2005) 5474–5491 https://doi.org/10.1016/j.biomaterials.2005.02.002.
48. F.S. Kaplan, W.C. Hayes, T.M. Keaveny, A. Boskey, T.A. Einhorn, J.P. Iannotti, Form and Function of Bone, Orthopaedic Basic Science, American Academy of Orthopaedic Surgeons, 1994, pp. 128–184.
49. T.M. Keaveny, E.F. Morgan, G.L. Niebur, O.C. Yeh, Biomechanics of trabecular

bone, Annu. Rev. Biomed. Eng. 3 (2001) 307–333 https://www.annualreviews.org/doi/abs/10.1146/annurev.bioeng.3.1.307.
50. G.A.P. Renders, L. Mulder, L. J van Ruijven, T.M.G.J. van Eijden, Porosity of human mandibular condylar bone, J. Anat. 3 (2010) 239–248 https://doi.org/10.1111/j.1469-7580.2007.00693.x.
51. J. Wieding, T. Lindner, P. Bergschmidt, R. Bader, Biomechanical stability of novel mechanically adapted open-porous titanium scaffolds in metatarsal bone defects of sheep, Biomaterials 46 (2015) 35–47 https://doi.org/10.1016/j.biomaterials.2014.12.010.
52. J. Wieding, A. Jonitz, R. Bader, The effect of structural design on mechanical properties and cellular response of additive manufactured titanium scaffolds, Materials 5 (2012) 1336–1347 https://doi.org/10.3390/ma5081336
53. Y. Kuboki, H. Takita, D. Kobayashi, E. Tsuruga, M. Inoue, M. Murata, et al., BMPinduced osteogenesis on the surface of hydroxyapatite with geometrically feasible and nonfeasible structures: topology of osteogenesis, J. Biomed. Mater. Res. 39 (1998) 190–199 https://doi.org/10.1002/(SICI)1097-4636(199802)39:2<190::AID-JBM4>3.0.CO;2-K.
54. Q. Chen, O. Bretcanu, A.R. Boccaccini, Inorganic and composite bioactive scaffolds for bone tissue engineering, in: P.K. Chu, X. Liu (Eds.), Biomaterials Fabrication and Processing Handbook, CRC Press, 2008.
55. A. Vahidgolpayegani, C. Wen, P. Hodgson, Y. Li, 2 - production methods and characterization of porous Mg and Mg alloys for biomedical applications, Metallic Foam Bone, 2017, pp. 25–82 https://doi.org/10.1016/B978-0-08-101289-5.00002-0.
56. Q. Ran, W. Yang, Y. Hu, X. Shen, Y. Yu, Y. Xiang, K. Cai, Osteogenesis of 3D printed porous Ti6Al4V implants with different pore sizes, Journal of the Mechanical Behavior of Biomedical Materials 84 (2018) 1–11 https://doi.org/10.1016/j.jmbbm.2018.04.010.
57. A.J. van den Bogert, Analysis and simulation of mechanical loads on the human musculoskeletal system: a methodological overview, Exerc. Sport Sci. Rev. 22 (1994) 23–51.
58. M. Fousová, D. Vojtěch, J. Kubásek, E. Jablonská, J. Fojt, Promising characteristics of gradient porosity Ti-6Al-4V alloy prepared by SLM process, Journal of the Mechanical Behavior of Biomedical Materials 69 (2017) 368–376 https://doi.org/10.1016/j.jmbbm.2017.01.043.
59. C. Wen, M. Mabuchi, Y. Yamada, K. Shimojima, Y. Chino, T. Asahina, Processing of biocompatible porous Ti and Mg, Scripta Mater. 45 (2001) 1147–1153.
60. C. Wen, Y. Yamada, K. Shimojima, Y. Chino, H. Hosokawa, M. Mabuchi, Novel titanium foam for bone tissue engineering, J. Mater. Res. 17 (2002) 2633–2639.
61. C. Wen, Y. Yamada, K. Shimojima, Y. Chino, T. Asahina, M. Mabuchi, Processing and mechanical properties of autogenous titanium implant materials, J. Mater. Sci. Mater. Med. 13 (2002) 397–401.

62. C. Wen, Y. Yamada, K. Shimojima, Y. Chino, H. Hosokawa, M. Mabuchi, Compressibility of porous magnesium foam: dependency on porosity and pore size, Mater. Lett. 58 (2004) 357–360.
63. L.G. Gibson, M.F. Ashby, Cellular Solids: Structure and Properties, second ed., Cambridge University Press, Cambridge, U.K, 1997, p. 429.
64. E.A. Lord, A.L. Mackay, S. Ranganatan, New Geometry for New Materials, Cambridge University Press, 2006.
65. M.M. Sychov, L.A. Lebedev, S.V. Dyachenko, L.A. Nefedova, Mechanical properties of energy-absorbing structures with triply periodic minimal surface topology, Acta Astronaut. (2017) 1–4 https://doi.org/10.1016/j.actaastro.2017.12.034.

66. D.J. Yoo, Porous scaffold design using the distance field and triply periodic minimal surface models, Biomaterials 32 (2011) 7741–7754 https://doi.org/10.1016/j.biomaterials.2011.07.019.
67. Mechanical properties of ceramic structures based on Triply Periodic Minimal Surface (TPMS) processed by 3D printing S Restrepo1, S Ocampo1, J A Ram´ırez1, C Paucar1 and Garc´ıa1 1 Universidad Nacional de Colombia, Medell´ın, Colombia To cite this article: S Restrepo *et al* 2017 *J. Phys.: Conf. Ser.* **935** 012036

68. Advanced lattice support structures for metal additive manufacturing DOI: 10.1016/j.jmatprotec.2013.01.020

69. Sikavitsas, V.I., Temenoff, J.S., Mikos, A.G., 2001. Biomaterials and bone mechanotransduction. Biomaterials 22, 2581–2593.

70. Ti–6Al–4V triply periodic minimal surface structures for bone implants fabricated via selective laser melting ChunzeYana,b,n, LiangHaob,n, AhmedHusseinb, PhilippeYoungb http://dx.doi.org/10.1016/j.jmbbm.2015.06.024

71. Sevilla, P., Aparicio, C., Planell, J.A., Gil, F.J., 2007. Comparison of the mechanical properties between tantalum and nickel- titanium foams implant materials for bone in growth applications. J. Alloy. Compd. 439, 67–73.

CERTIFICATE OF COMPLETENESS

It is hereby certified that the dissertation submitted by *NS Hamza Ali*, Registration No.00000205033, Titled: "FE modelling of porous structures using Selective laser melting" has been checked/reviewed and its contents are complete in all respects.

Signature of Supervisor

(Dr. Khalid Mahmood)